Precision Measurements of π^0 Electroproduction near Threshold: A Test of Chiral QCD Dynamics

$$p(\vec{e},e'p)\pi^0$$

E04-007 Experiment

contributed by R. Lindgren
for
J.R.M. Annand, **K. Chirapatimol**, D.W. Higinbotham, R. Lindgren, N. Liyanage,
B. Moffit, B. Norum,
V. Nelyubin, M. Shabestari and **C. Smith**
and
The BigBite and Hall-A Collaboration

Chiral Dynamics Conference
Jefferson Lab
2012

Jefferson Lab

Outline

- Motivation
- JLAB Experiment E04-007
- Analysis Goals
- Extracted Legendre Polynomial Coefficients
- Systematic Errors
- Comparison with Mainz
- Conclusions

Chiral Dynamics Effective Theory

- A low energy effective field theory that uses a Lagrangian that is invariant under the symmetry transformations of QCD.
  - Exact for charge, parity, time reversal symmetries
  - Approximate for flavor and chiral symmetry

  (Last two are exact for massless quarks)

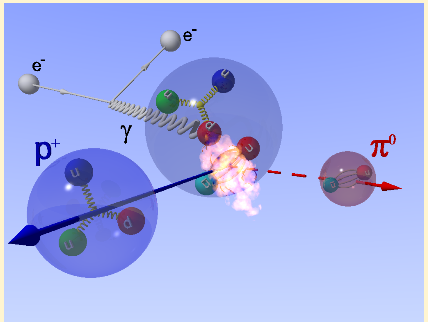

- Expand the Lagrangian in terms of hadron-pion interactions in terms of ratios of q/M. Infinite number of terms. At low Q^2 you can calculate and sum over relevant diagrams and represent uncalculable terms by low energy constants

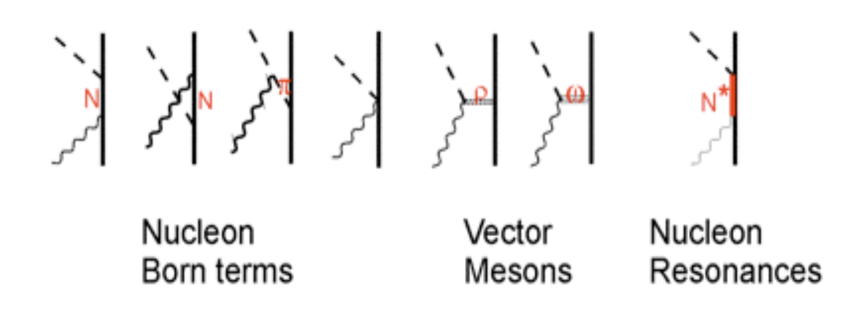

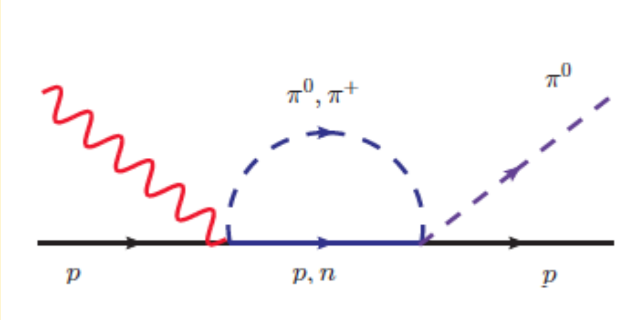

- Once the LEC's are determined, one can predict the evolution of the electroproduction cross section and pion amplitudes with energy and momentum (W, Q^2..)

  Extend data to test HBCHPT at higher W and Q^2

Previous p(e,e'p)π^0 Data from Mainz

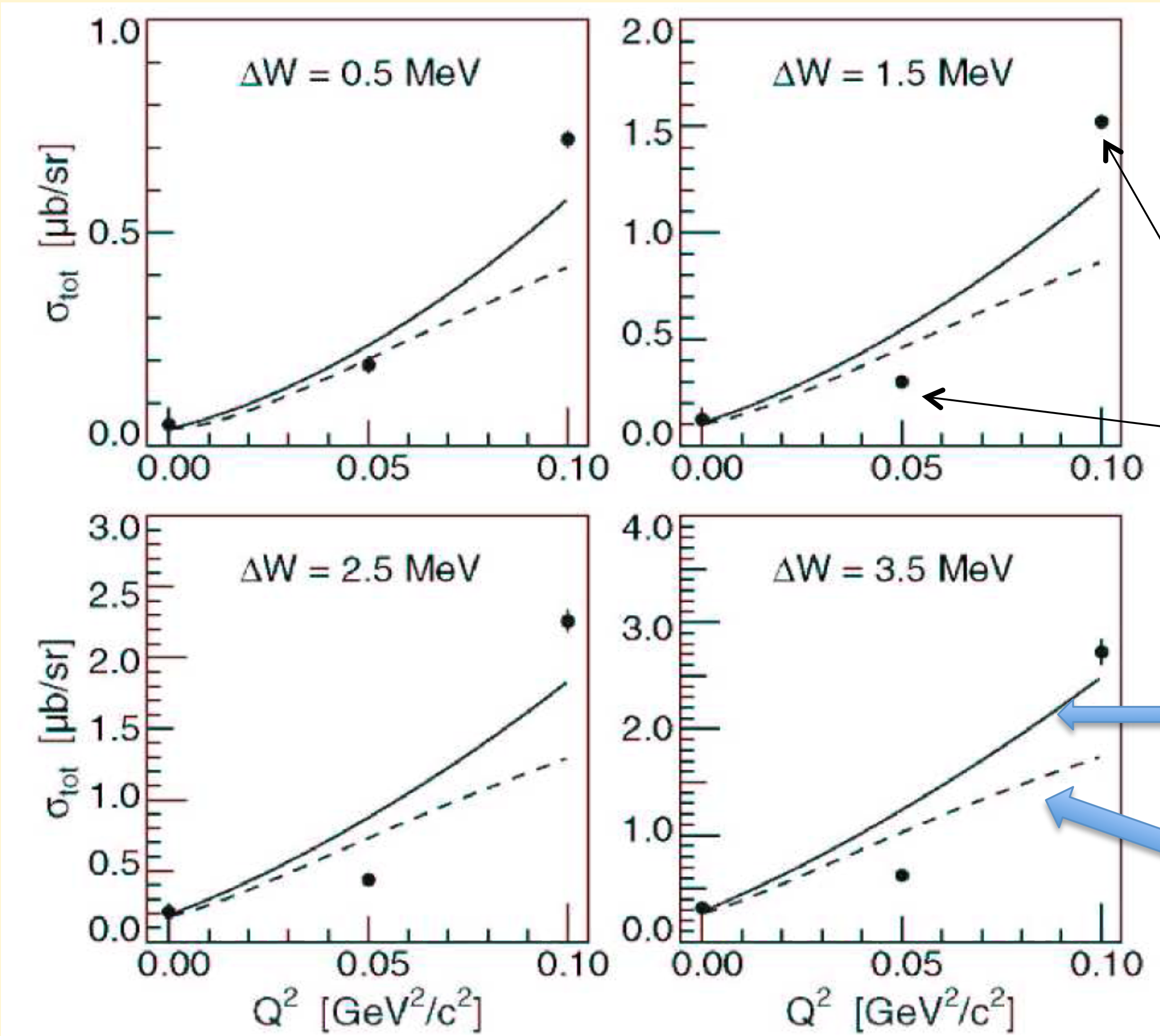

LEC's (from Q^2 = 0.10 GeV^2)
a_3 = - 0.92 and a_4 = - 0.99

Q^2=0.10 $(GeV/c)^2$
Distler PRL 80, 2294 (1998)

Q^2=0.05 $(GeV/c)^2$
Merkel et al. PRL 88, 1230 (2002)

HBChPT ——
Bernard al. NP A607,379(1996)

MAID - - -

Significant discrepancy between experiment and theory.

Situation in 2002.

Kinematic Coverage of Data
JLAB Experiment E04-007

$p(\vec{e},e'p)\pi^0$ Proton Electron

beam energy(GeV)	$\theta_{BB}(deg)$	$\theta_{HRS}(deg)$
1.192	-54.0	35.5
		20.5
		16.5
		14.5
		12.5
	-48.0	27.0
		20.5
		16.5
		14.5
		12.5
	-43.5	20.5
		16.5
		14.5
		12.5
2.323	-54.0	13.2
		15.8
		18.2

1) $E = 1.192\ GeV$

$0 \le \Delta W \le 30\ MeV$

$0.05 \le Q^2 \le 0.15\ (GeV/c)^2$

$Bin\ \Delta W\ \ in\ 1MeV$

$Bin\ Q^2\ \ in\ 0.01\ (GeV/c)^2$

2) $E = 2.323\ GeV$

$0 \le \Delta W \le 60\ MeV$

$0.20 \le Q^2 \le 0.50\ (GeV/c)^2$

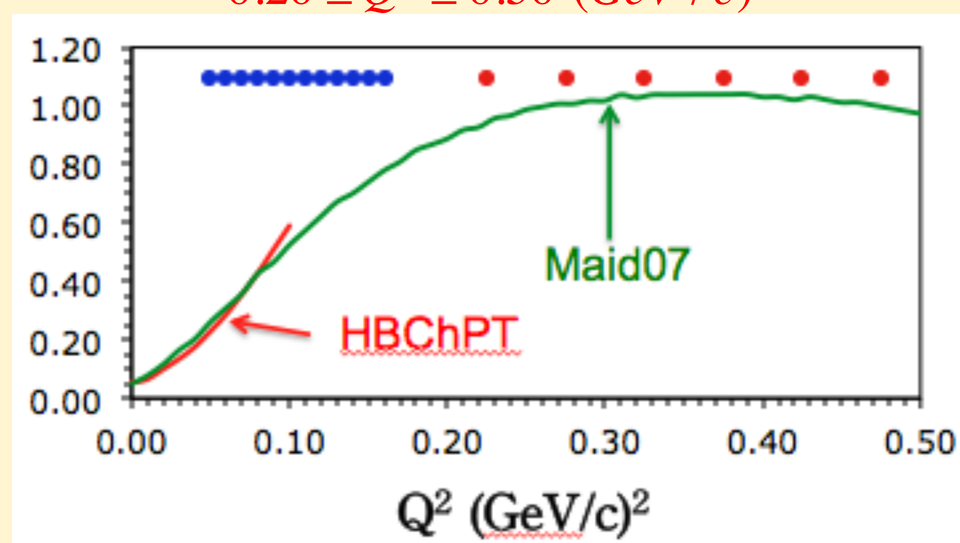

Jefferson Lab

E04-007: Experimental Setup in Hall A

$$p(\vec{e},e'p)\pi^0$$

LH2 Target Cell
- 6 cm long, 1” diameter
- 200 μm 7075 Al Foil

Vacuum Scattering Chamber

Electron Beam
- E=1.192 GeV
- 1-7 μA

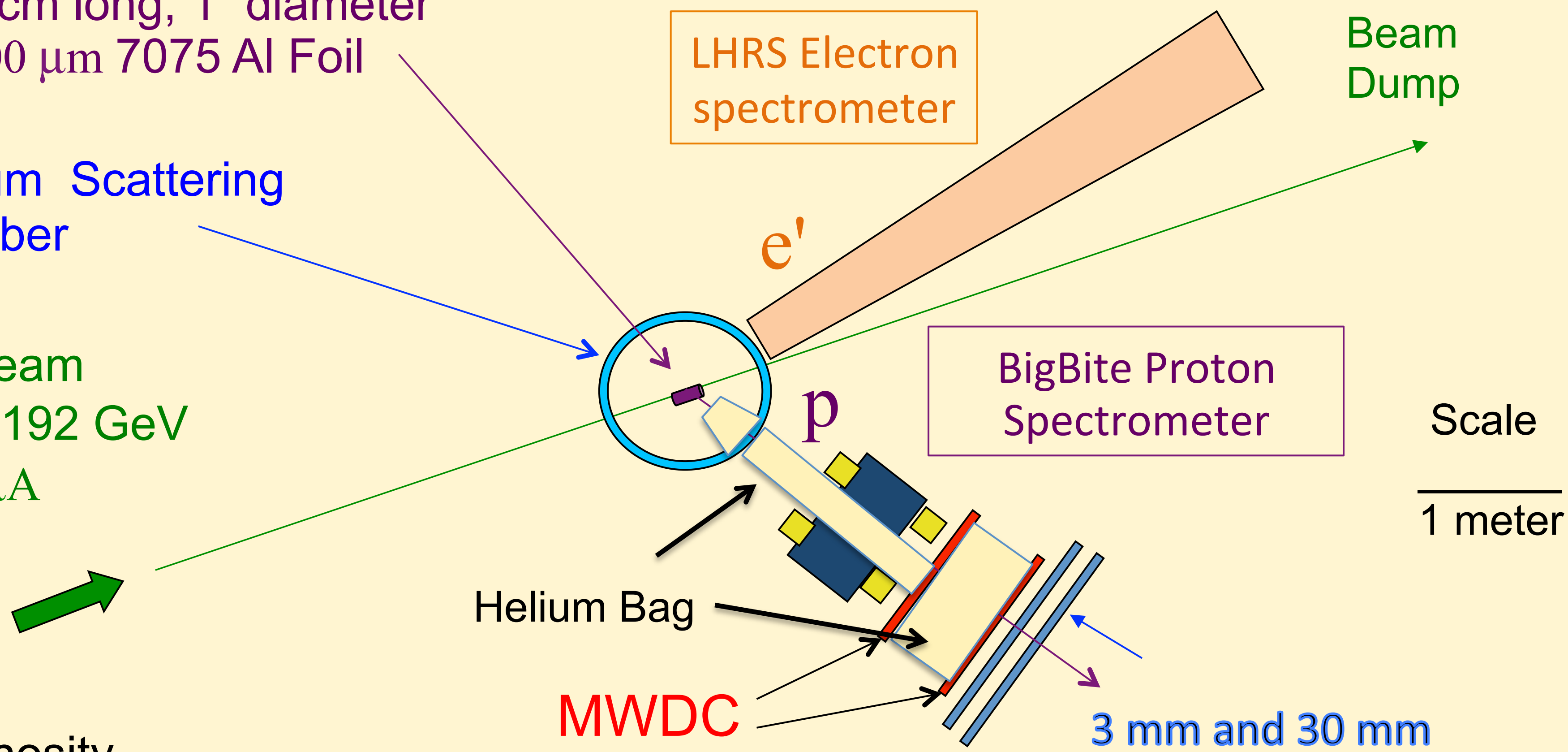

Luminosity
- 1 x 10^{37} Hz/cm^2

Multi Wire Drift Chambers (MWDC)
- Low mass and thickness minimizes straggling for low energy protons

Jefferson Lab

Proton Arm

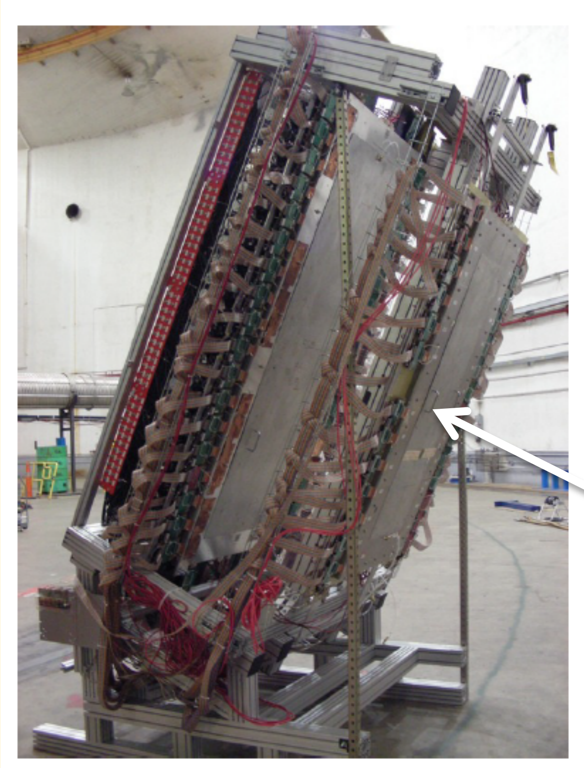

BigBite Detector Package (Helium bag removed)

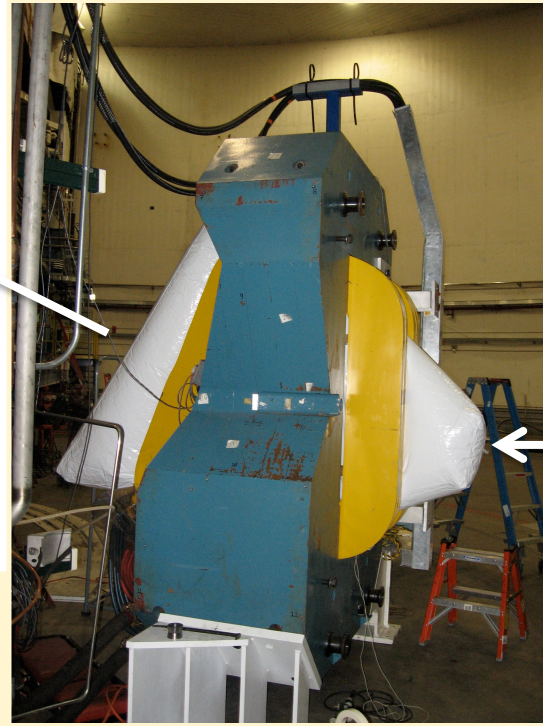

BigBite
Non-focussing
_normal-conducting
dipole magnet
100 msr
0.2 – 0.9 GeV/c
1 Tesla

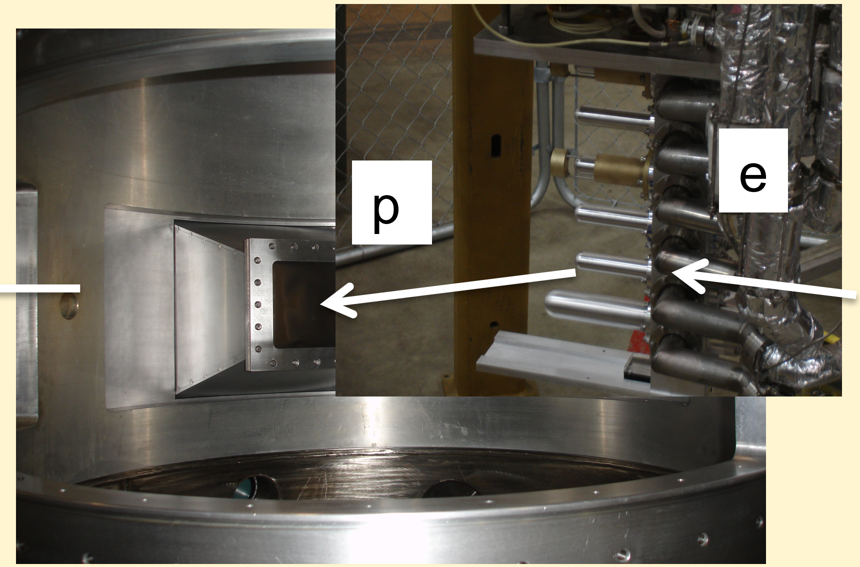

Cryo-Target System and solid target ladder

Target System

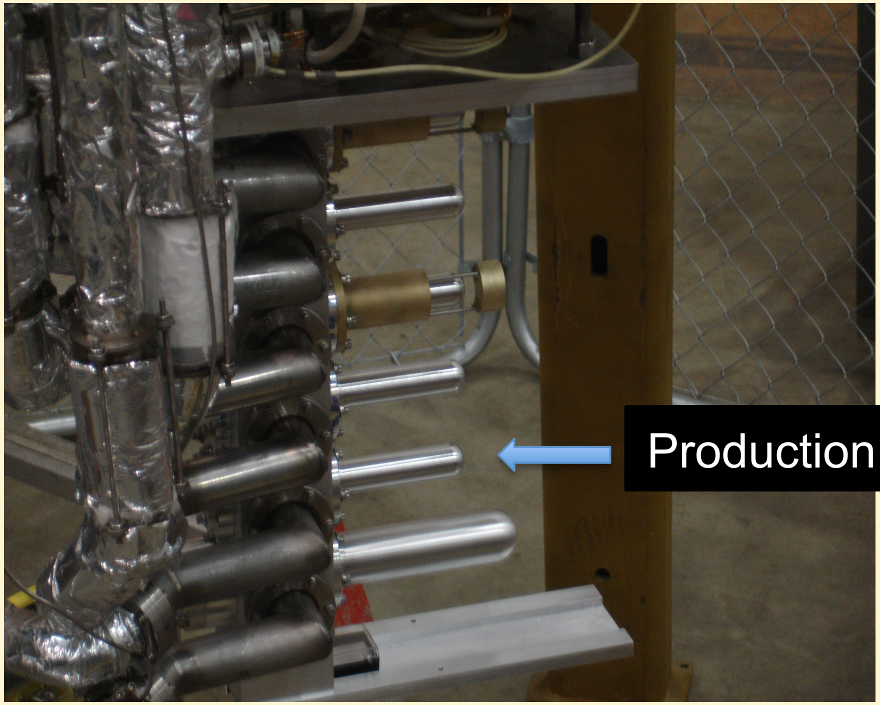

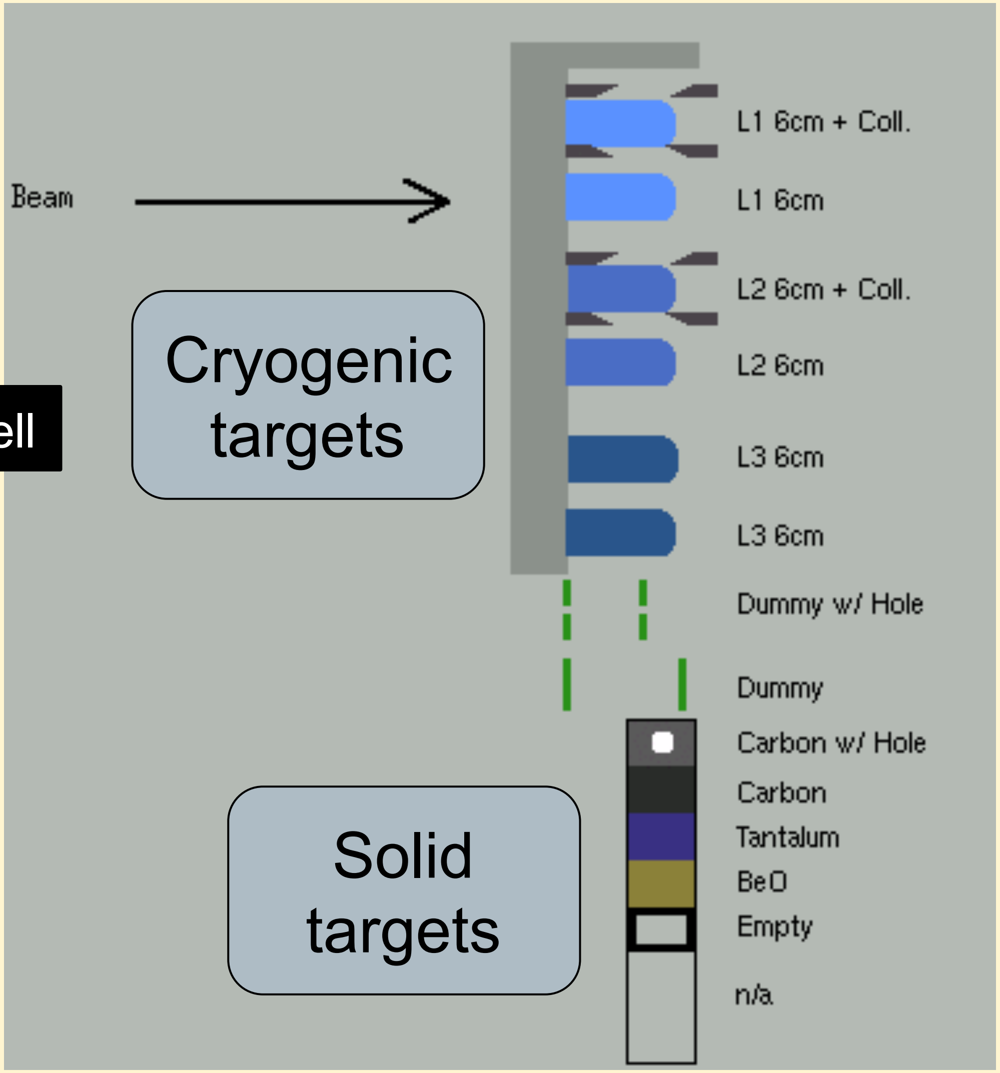

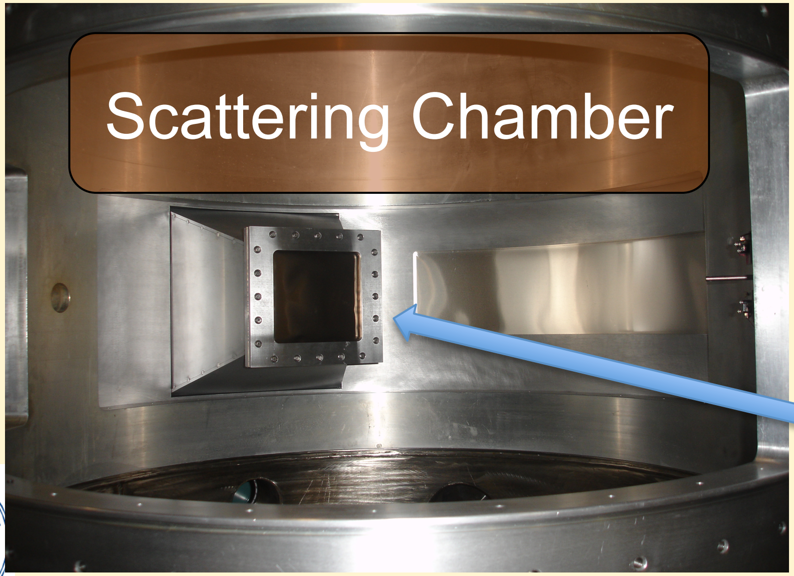

Inset Flange with 0.003" Ti Window

Jefferson Lab

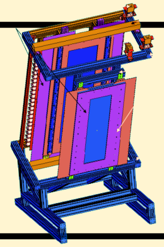

BigBite Spectrometer

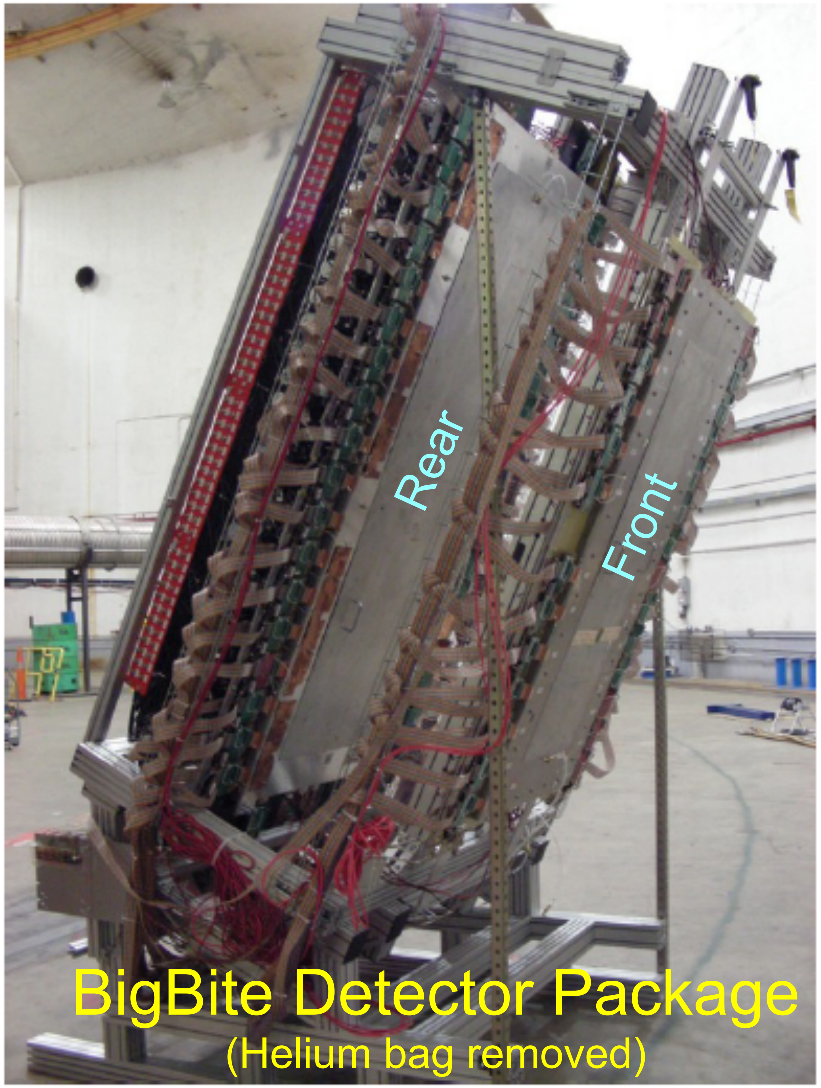

Proton Tracking:

- Front MWDC (6 planes) 35 x 140 cm^2
- Rear MWDC (6 planes) 50 x 200 cm^2
- Designed for high rate capability and resolution with unambiguous track reconstruction

Proton Trigger and PID:

- Two 24 paddle scintillator planes
- ΔE: 3 mm, E: 30 mm

Proton identification relies on combination of energy deposition and TOF from BB•LHRS coincidence trigger

Jefferson Lab

BigBite Magnet with Helium Bag

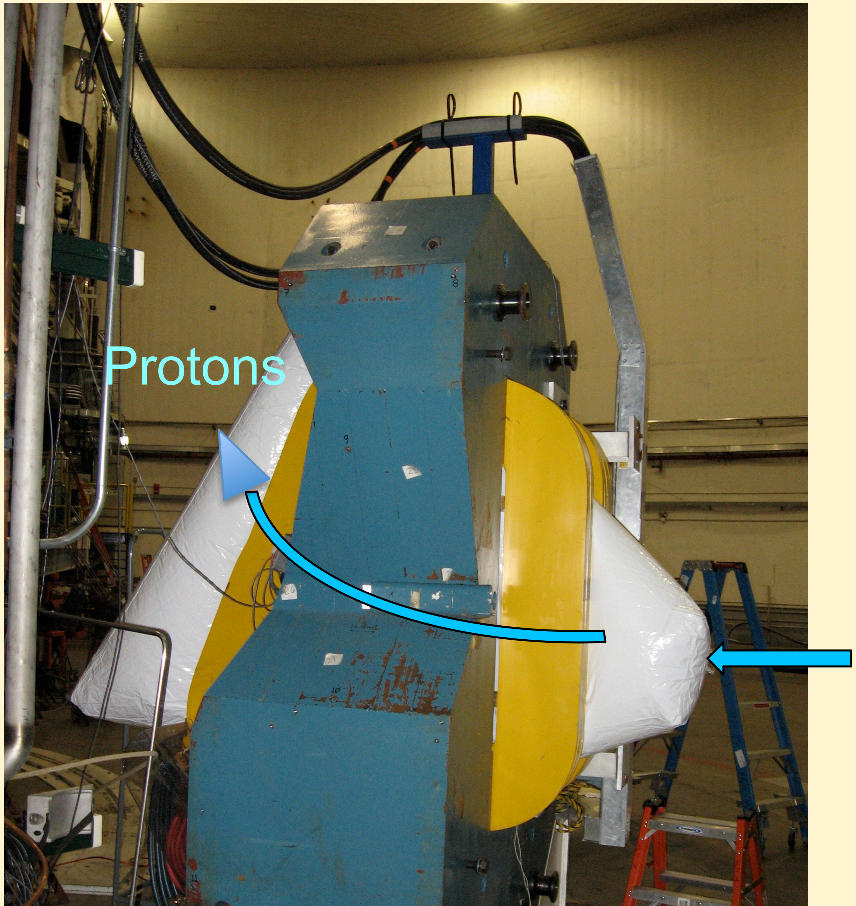

Helium filled polyurethane balloons to minimize energy loss and multiple scattering
Thickness 0.0035″

Non-focussing normal-conducting dipole magnet spectrometer

Combines a **large solid angle** with a **large momentum acceptance.**

Field strength ~1 Tesla

Main design characteristics of BigBite [15]	
Configuration	Dipole
Momentum range	$200 - 900$ MeV/c
Momentum acceptance	$-0.6 \leq \frac{\delta p}{p} \leq 0.8$
Momentum resolution	4×10^{-3}
Angular acceptance	≈ 100 msr
Angular resolution	≈ 1 msr

Magnet field map calculated using TOSCA

Jefferson Lab

Helium Bags

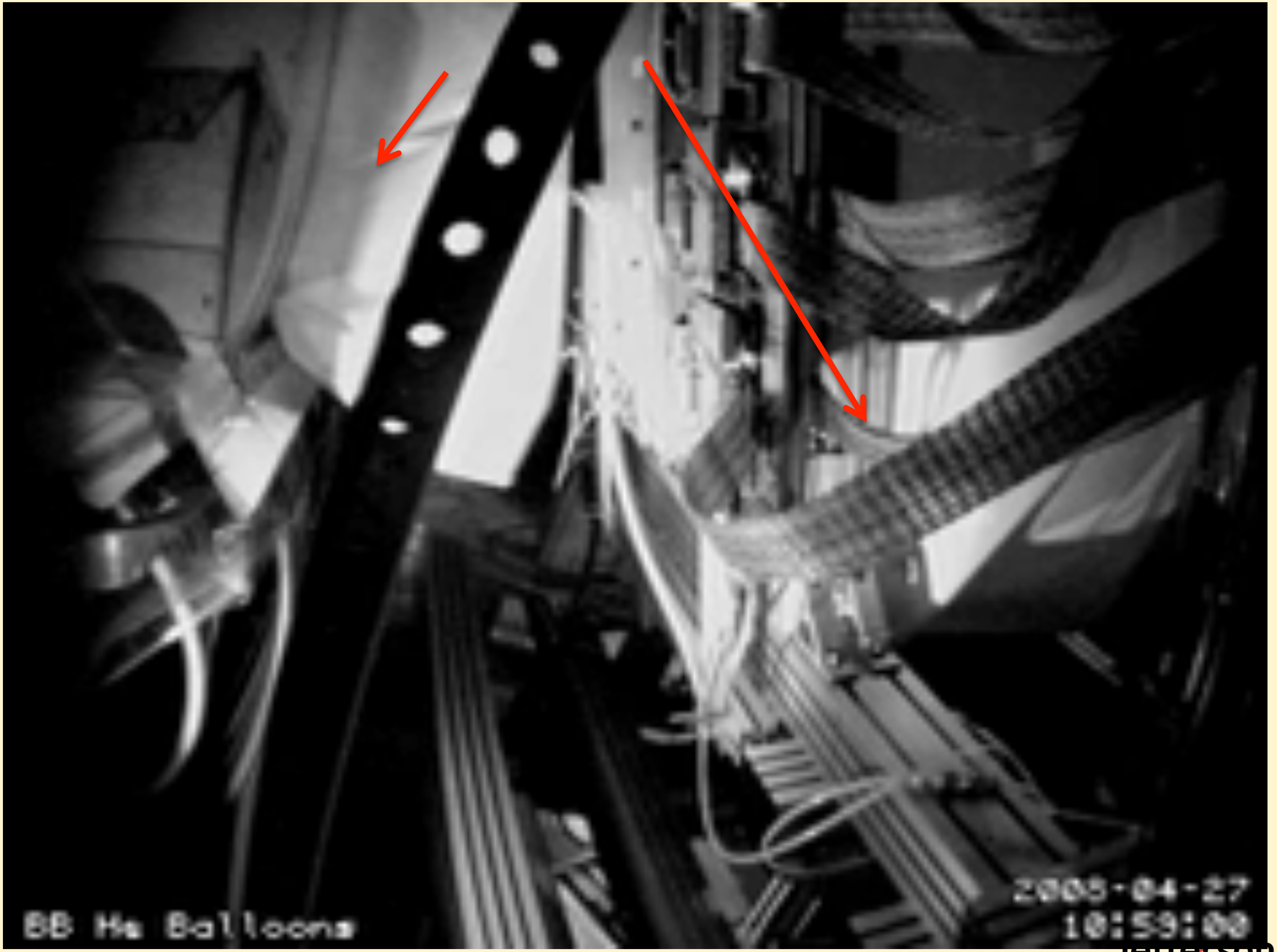

Jefferson Lab

E04-007 Spectrometers

Main design characteristics of HRS's [14]	
Configuration	QQDQ
Momentum range	0.3 – 4.0 GeV/c
Momentum acceptance	$-4.5\% \leq \frac{\delta p}{p} \leq 4.5\%$
Momentum resolution	1×10^{-4}
Angular acceptance	
Horizontal	±30 mrad
Vertical	±60 mrad
Angular resolution	
Horizontal	0.5 mrad
Vertical	1.0 mrad

$$Q^2 == 4EE' \sin^2(\frac{\theta_e}{2})$$

$$W^2 = M_p^2 + 2M_p(E_e - E_e^{'}) - Q^2$$

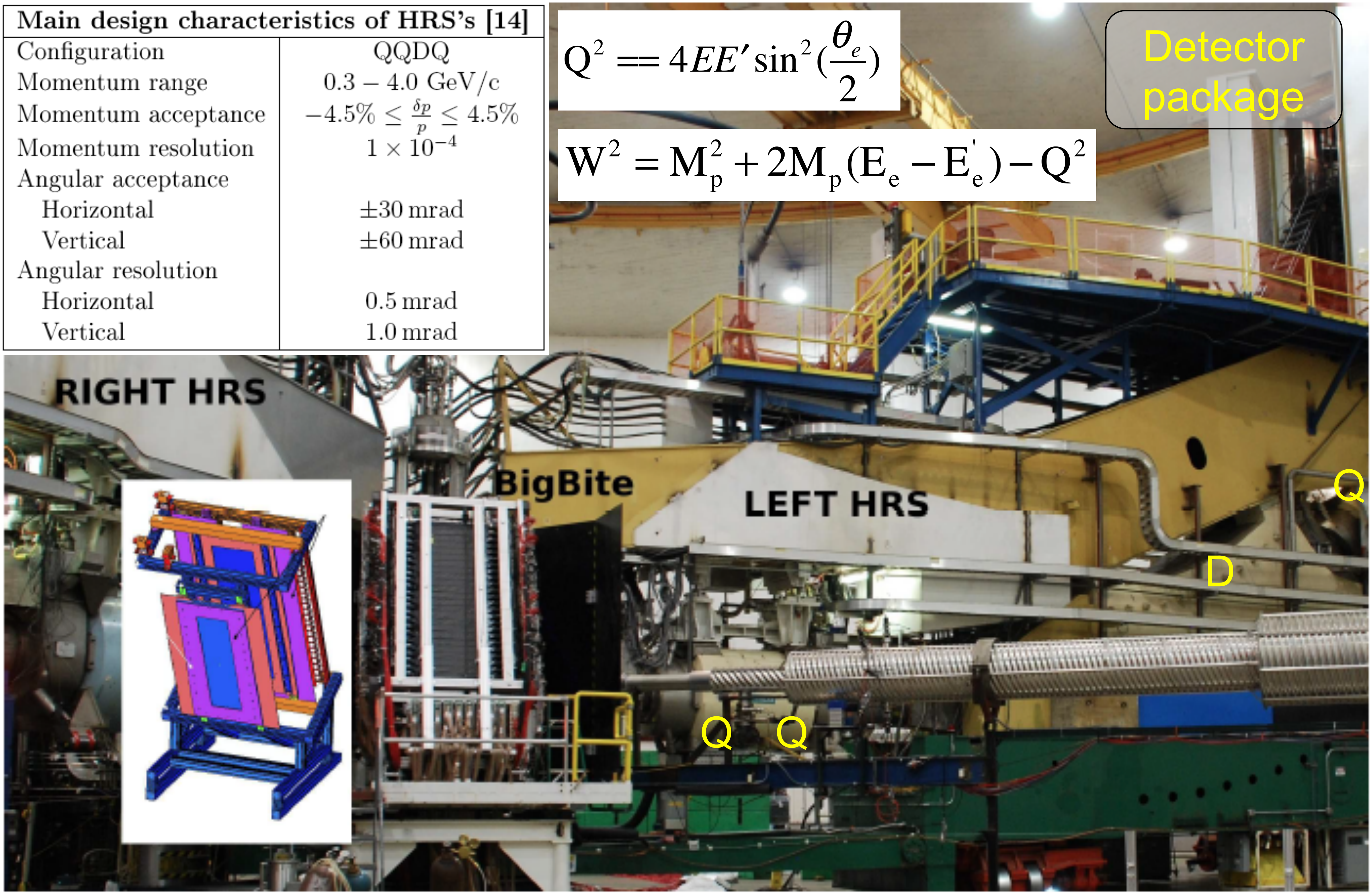

E04-007: Coincidence Kinematics

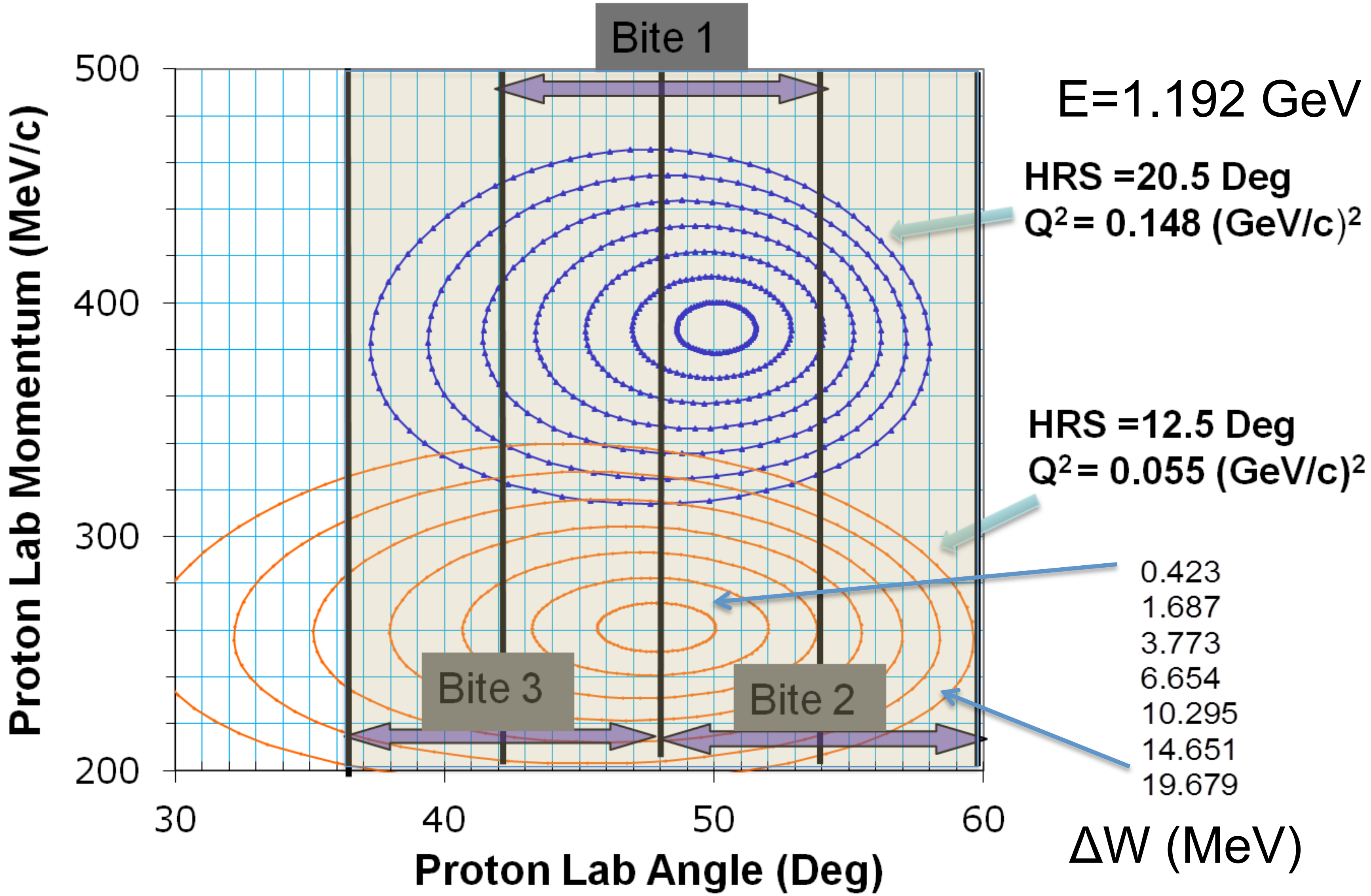

Ellipses of constant ΔW (W relative to π threshold)

Jefferson Lab

Constant W Ellipses in BigBite Data Compared to Simulation using DMT Physics Model ΔW=19-21 MeV

Lab Proton Momentum GeV/c

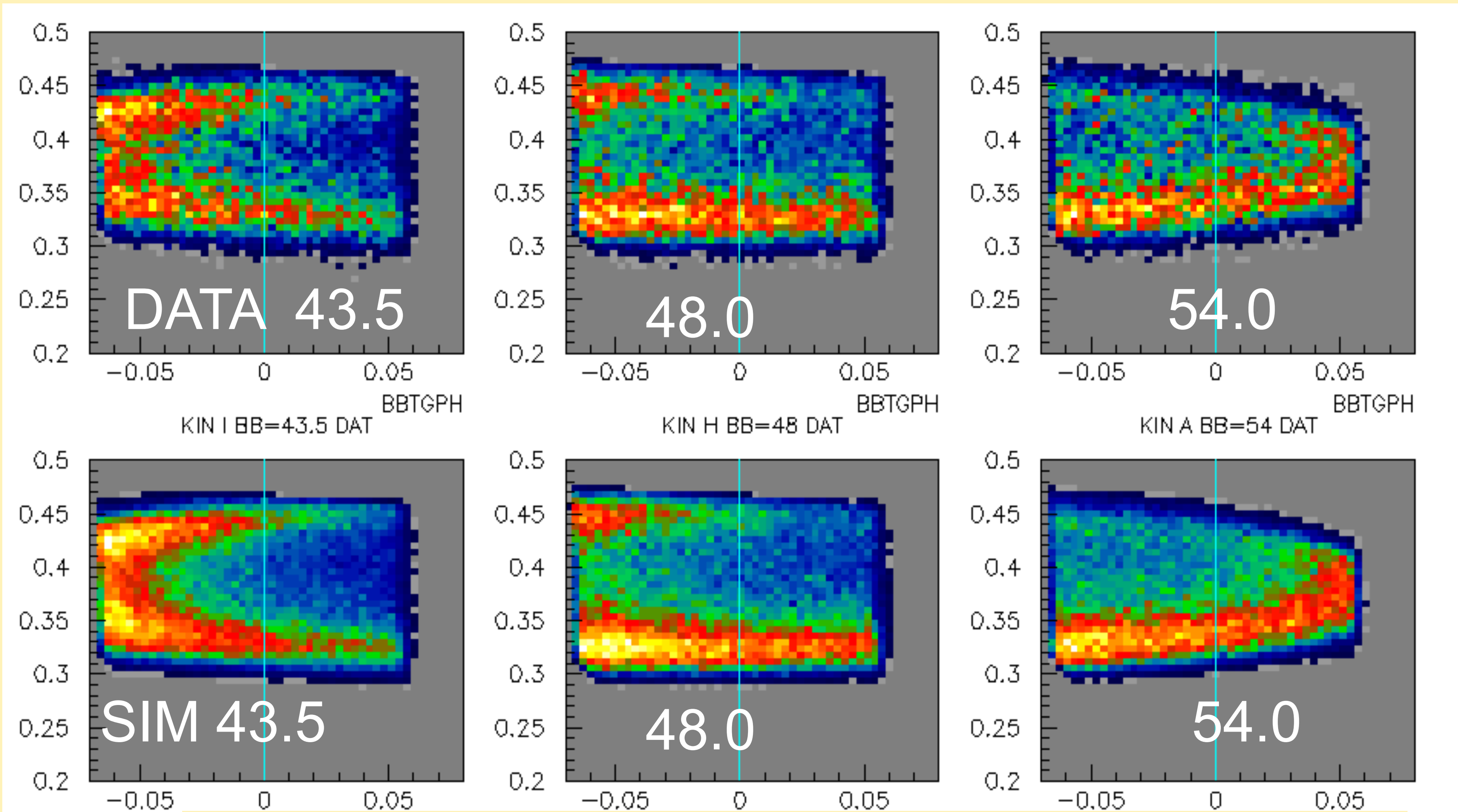

BigBite Target proton Angle (Lab)

Missing Mass Spectrum

Blue points show final missing mass distribution after subtraction of target cell windows.

Contribution from windows shown by red curve.

Nominal missing mass cut was +/- 10 MeV with respect to 135 MeV.

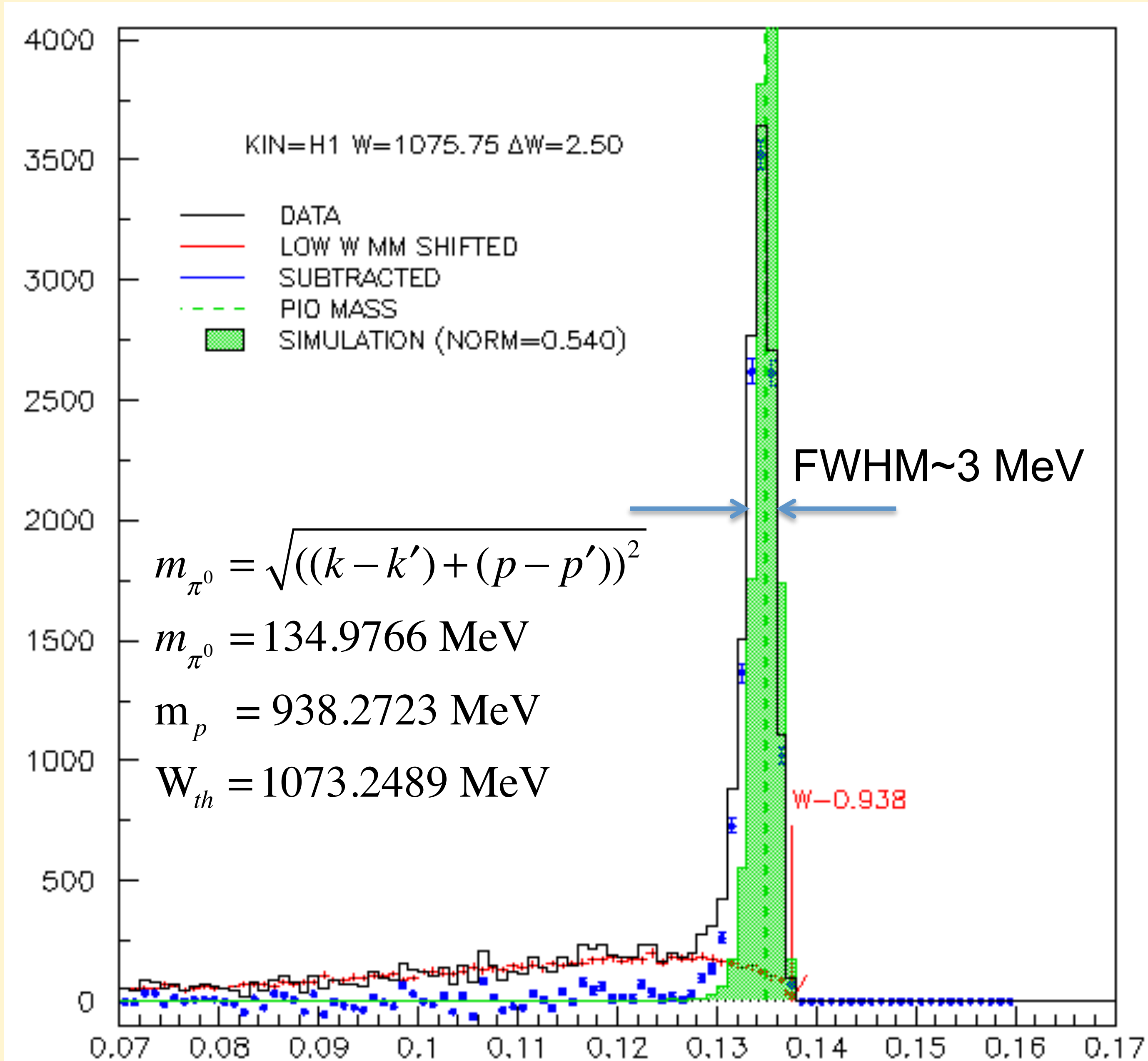

Missing Mass (GeV)

Jefferson Lab

Converting Yield Y to Cross Section from the Data

$$\frac{d^5\sigma}{dQ^2 dW d\phi_e d\Omega_\pi^*} = \frac{Y}{\Delta Q^2 \Delta W \Delta\phi_e \Delta\Omega_\pi^*} \frac{eA}{N_A \rho t C \varepsilon (1-D) R} \frac{1}{f_{Acc}}$$

$$f_{Acc} = \frac{\text{Number of thrown events that pass all acceptance cuts}}{\text{Number of thrown events}}$$

$$\frac{d^5\sigma}{d\Omega_e d\Omega_\pi^* dE'} = \frac{d\sigma}{dQ^2 dW d\phi_e d\Omega_\pi^*} \frac{1}{J} \qquad J = \frac{W}{2mEE'}$$

J is Jacobian to transfer from $(\cos\theta_e, E')$ to (Q^2, W) variables

Jefferson Lab

Cross Section vrs Φ^*_π and Cos θ^*_π and Legendre Polynomial Coefficients

- Cross Section Matrix of data
- Q^2 along the top
- W along the left side edge
- http://galileo.phys.virginia.edu/~lcs1h/halla/yld4e.html
- **Preliminary Results (Not for distribution)**

Analysis Goals I

Extract 4 structure functions for each W and Q^2 point using measured φ* distributions and compare with previous MAMI experiments and HChPT, MAID07 and DMT calculations.

$$\sigma_T(\theta_\pi^*) + \varepsilon_L \sigma_L(\theta_\pi^*)$$

$$\sigma_{LT}(\theta_\pi^*)$$

$$\sigma_{TT}(\theta_\pi^*)$$

$$\sigma_{LT'}(\theta_\pi^*)$$

$$\frac{d\sigma}{d\Omega_\pi^*} = \sigma_T(\theta_\pi^*) + \varepsilon_L \sigma_L(\theta_\pi^*) + \sqrt{2\varepsilon_L(1+\varepsilon)}\sigma_{LT}(\theta_\pi^*)\cos\phi_\pi^* + \varepsilon\sigma_{TT}(\theta_\pi^*)\cos 2\phi_\pi^* +$$

$$h\sqrt{2\varepsilon_L(1-\varepsilon)}\sigma_{LT'}(\theta_\pi^*)\sin\phi_\pi^*$$

Analysis Goals II

Extract *model independent* partial wave content of structure functions using Legendre polynomial fits (assume s,p-wave dominance.)

$$\frac{d^5\sigma}{dE_{e'}\,d\Omega_{e'}\,d\Omega_\pi^*} = \Gamma_v \frac{d\sigma}{d\Omega_\pi^*}$$

$$\frac{d\sigma}{d\Omega_\pi^*} = \frac{p_\pi^*}{k_\gamma^*}\left(A_0^{T+L} + A_1^{T+L}P_1(x) + A_2^{T+L}P_2(x)\right) \qquad \text{T+L}$$

$$+\frac{p_\pi^*}{k_\gamma^*}\sqrt{2\varepsilon_L(1+\varepsilon)}\left(A_0^{LT} + A_1^{LT}P_1(x)\right)(1-x^2)^{1/2}\cos\phi_\pi^* \qquad \text{LT}$$

$$+\frac{p_\pi^*}{k_\gamma^*}\varepsilon A_0^{TT}(1-x^2)\cos 2\phi_\pi^* \qquad \text{TT}$$

$$+h\frac{p_\pi^*}{k_\gamma^*}\sqrt{2\varepsilon_L(1-\varepsilon)}\left(A_0^{LT'} + A_1^{LT'}P_1(x)\right)(1-x^2)^{1/2}\sin\phi_\pi^* \qquad \text{LT'}$$

$$x = \cos(\theta_\pi^*) \quad h = beam\,helicity$$

Analysis Goals III

Perform model dependent fits to estimate electromagnetic multipoles, needed for precise comparison to models.

$$d\sigma_T = |E_{0+}|^2 + \frac{1}{2}\left(|P_2|^2 + |P_3|^2\right) + 2\,\mathrm{Re}\left(E_{0+}P_1^*\right)\cos\theta_\pi^* + \left(|P_1|^2 - \frac{1}{2}\left(|P_2|^2 + |P_3|^2\right)\right)\cos^2\theta_\pi^*$$

$$d\sigma_L = \left(|L_{0+}|^2 + |P_5|^2\right) + 2\,\mathrm{Re}\left(L_{0+}P_4^*\right)\cos\theta_\pi^* + \left(|P_4|^2 - |P_5|^2\right)\cos^2\theta_\pi^*$$

$$d\sigma_{TT} = \frac{1}{2}\left(|P_2|^2 - |P_3|^2\right)\sin^2\theta_\pi^*$$

$$P_1 = 3E_{1+} + M_{1+} - M_{1-} \quad P_2 = 3E_{1+} - M_{1+} + M_{1-}$$

$$P_3 = 2M_{1+} + M_{1-} \quad P_4 = 4L_{1+} + L_{1-} \quad P_5 = L_{1-} - 2L_{1+}$$

$$d\sigma_{LT} = -\mathrm{Re}\left(L_{0+}P_2^* + E_{0+}P_5^*\right)\sin\theta_\pi^* - \mathrm{Re}\left(P_1P_5^* + P_4P_2^*\right)\sin\theta_\pi^*\cos\theta_\pi^*$$

$$d\sigma_{LT'} = -\mathrm{Im}\left(L_{0+}P_2^* + E_{0+}P_5^*\right)\sin\theta_\pi^* + \mathrm{Im}\left(P_1P_5^* + P_4P_2^*\right)\sin\theta_\pi^*\cos\theta_\pi^*$$

LHRS=20.5° ΔW=9.5 MeV Q^2=0.135 (GeV/c)^2

—— Legendre Fit —— HBChPT (1996)

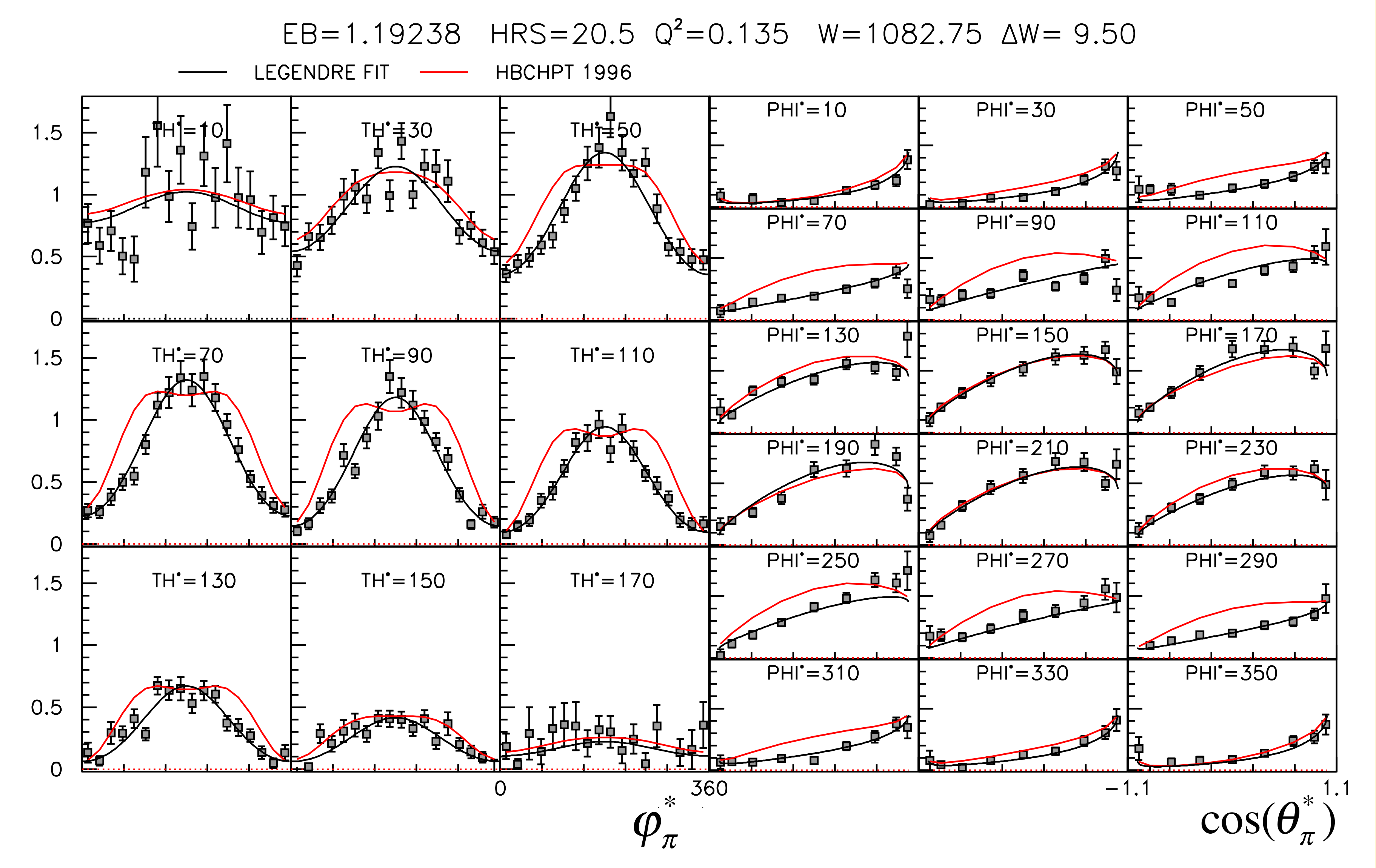

ΔW Dependence of A^{TT}_0

$$A_0^{TT} = \frac{1}{2}(|P_2|^2 - |P_3|^2)$$

— HBChPT
— DMT
— MAID07

■ JLAB 2012
■ MAMI 2011

H. Merkel et al.,
arXiv:1109.5075v1 [nucl-ex].

$$P_3^{Born+ct} = eq(\frac{g_{\pi n}}{16\pi m^3} + b_p)\sqrt{\omega^2 - k^2}$$

$$b_p = 13.0 \text{ x } 10^{-9} \text{ MeV}^{-3}$$

HBCHPT : $|P_3|^2 > |P_2|^2$

Data : $|P_3|^2 \approx |P_2|^2$

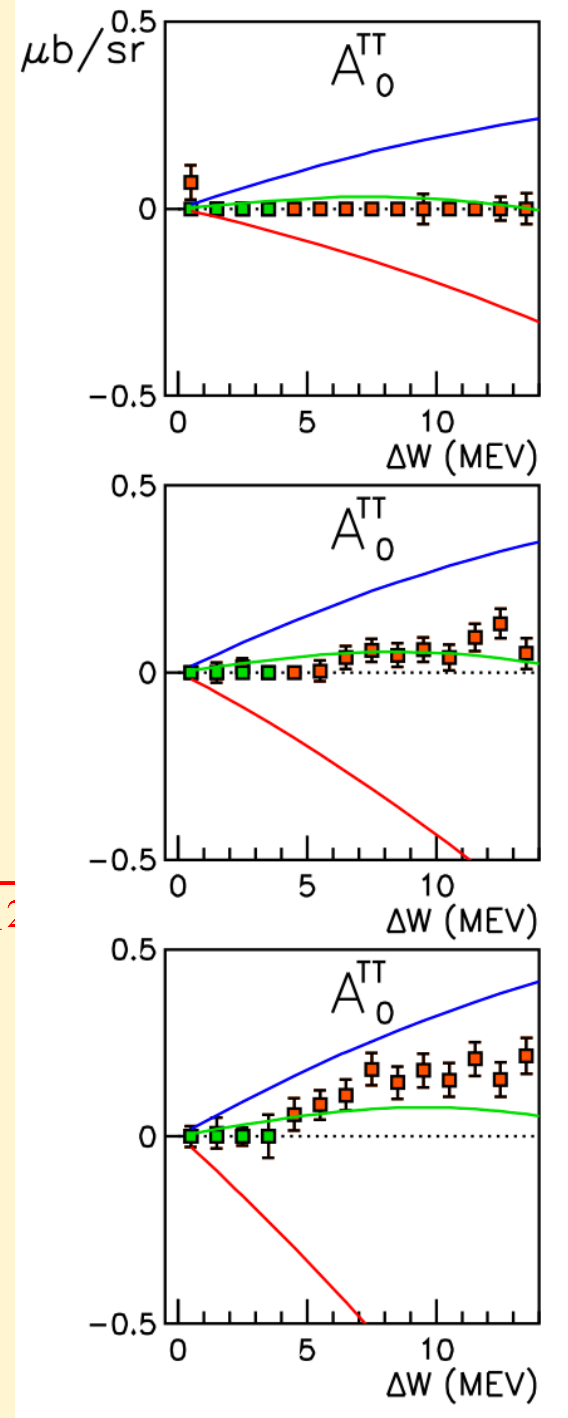

Q^2=0.05 (GeV/c)^2
(Consistent with zero)

Q^2=0.10 (GeV/c)^2

Q^2=0.15 (GeV/c)^2

Jefferson Lab

Q^2 Dependence of A_0^{TT}

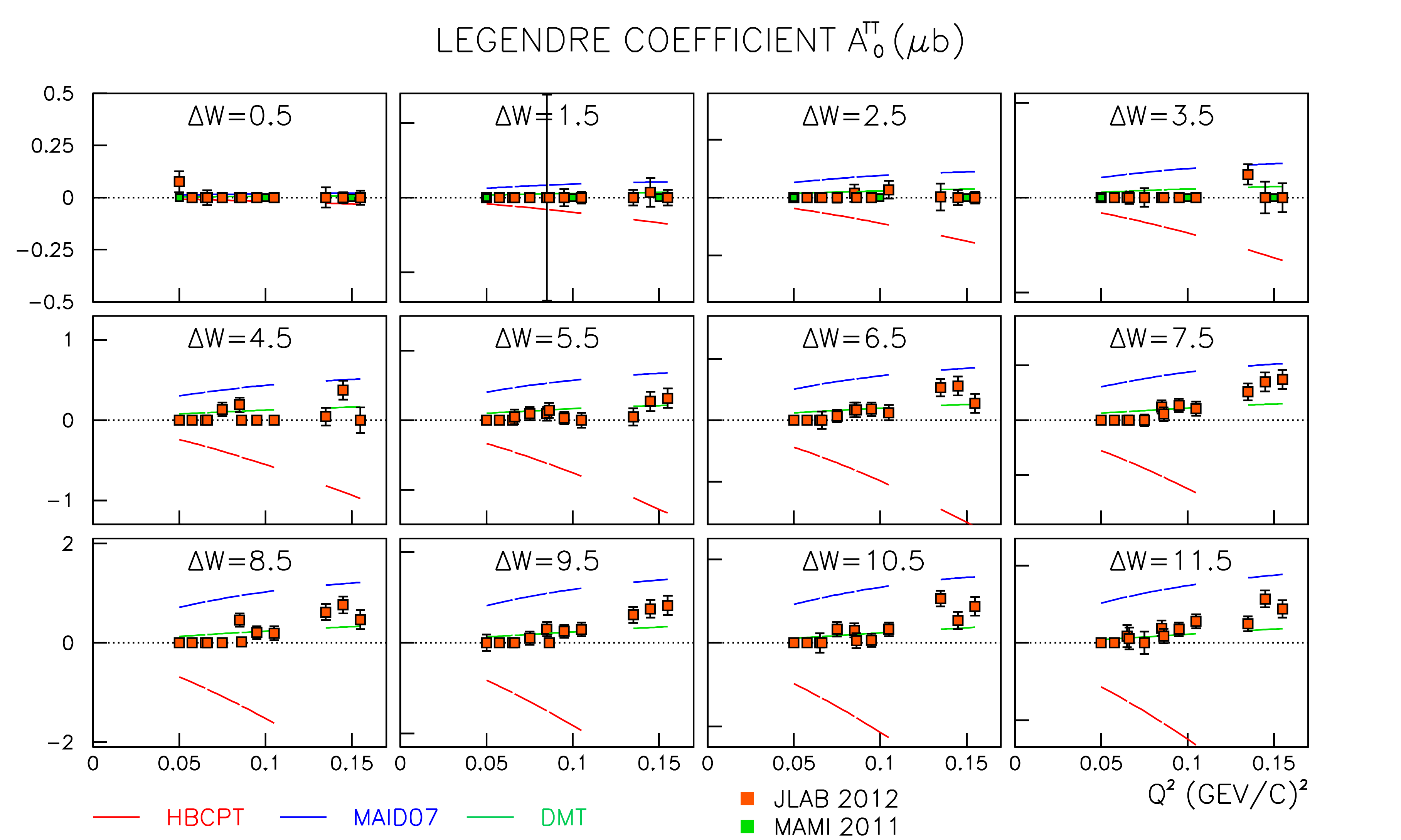

Both Q^2 and W dependence of σ_{TT} in strong disagreement with $O(q^3)$ ChPT. Changing b_p LEC to compensate may destroy agreement with other p-wave observables.

Jefferson Lab

ΔW Dependence of A^{T+L}

- HBChPT
- DMT
- MAID07

- JLAB 2012
- MAMI 2011

A^{T+L}

$A_0 \approx \sigma_{TOT}$

$A_1 \rightarrow \mathrm{Re}(E_{0+}P_1^*)$ dominates

$A_2 \rightarrow |P_2|^2 + |P_3|^2$ p-waves

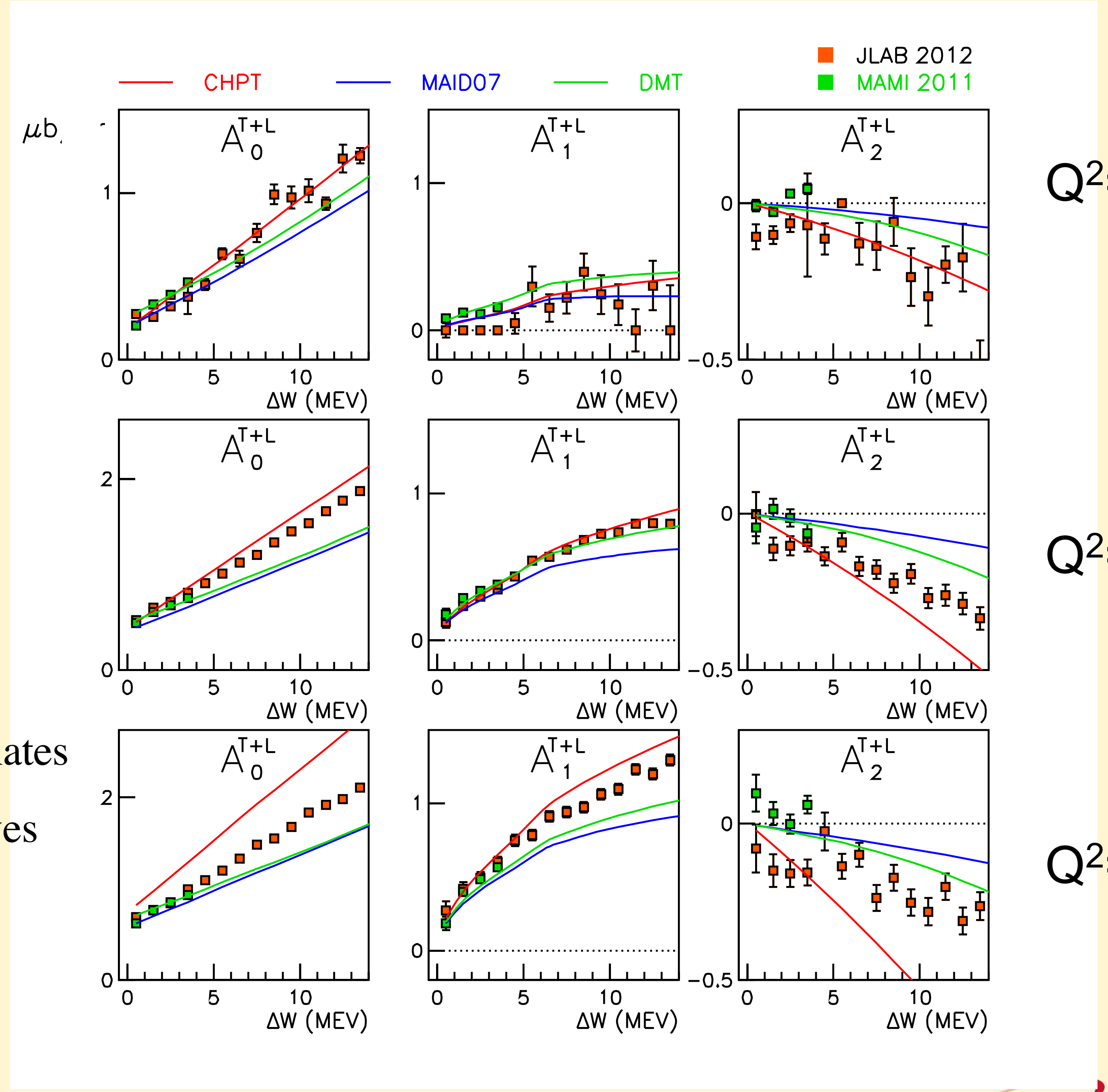

Q²=0.05

Q²=0.10

Q²=0.15

Jefferson Lab

Q^2 Dependence of A_0^{T+L} at 0.5 MeV Above Threshold

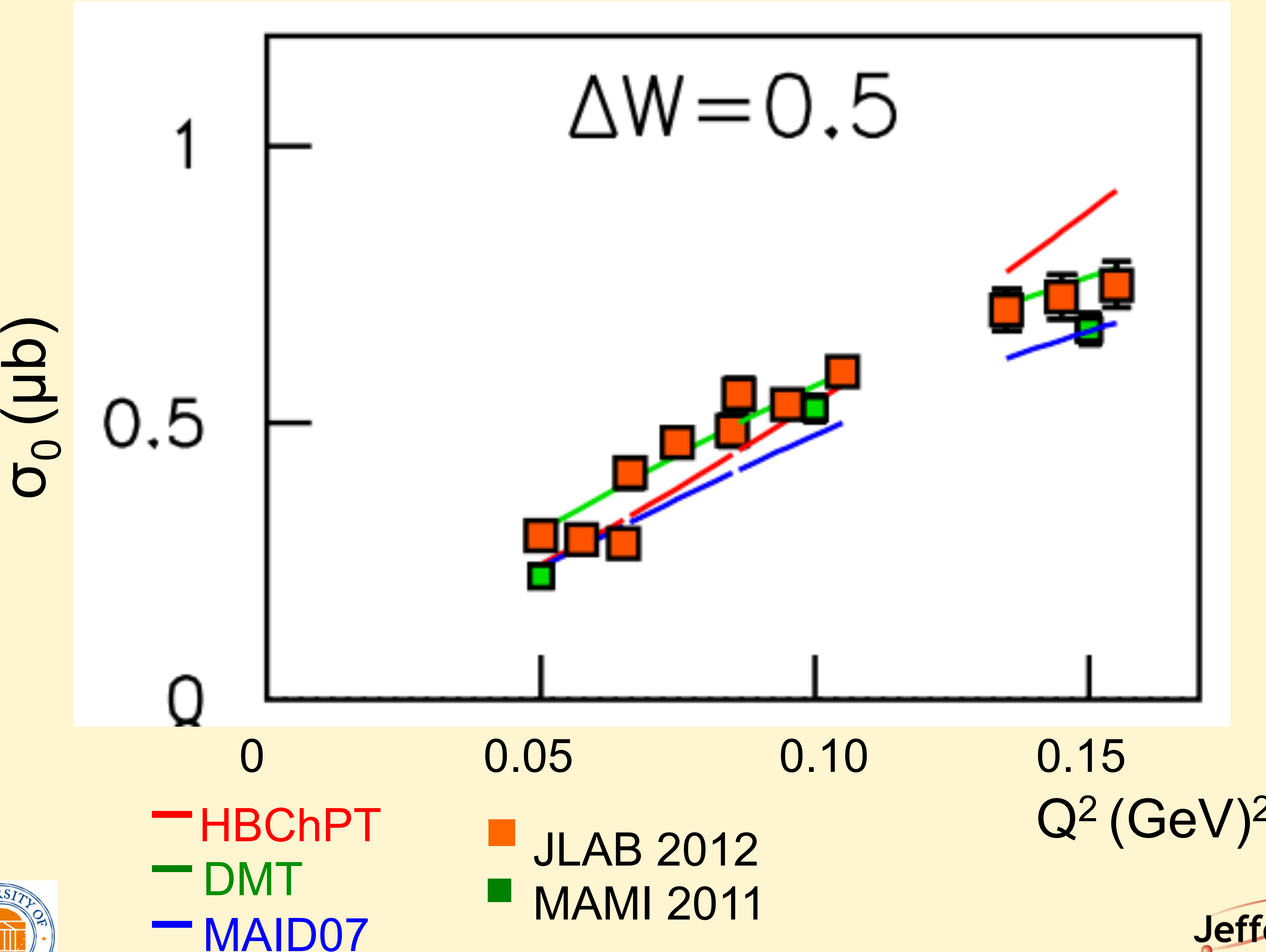

Q^2 Dependence of A_0^{T+L} 0.5 – 3.5 MeV

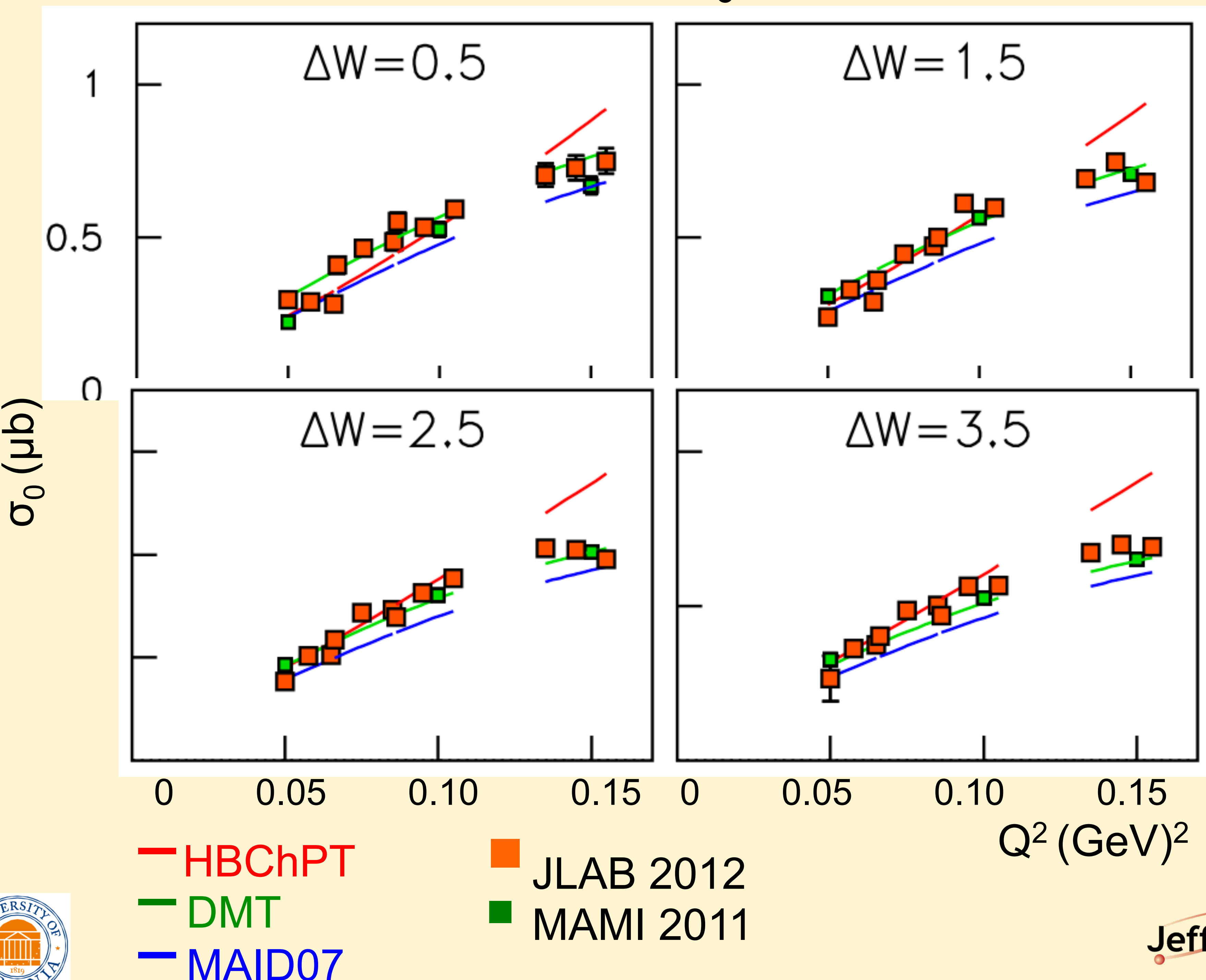

Jefferson Lab

Q^2 Dependence of A_0^{T+L} from 0.5 to 11.5 MeV

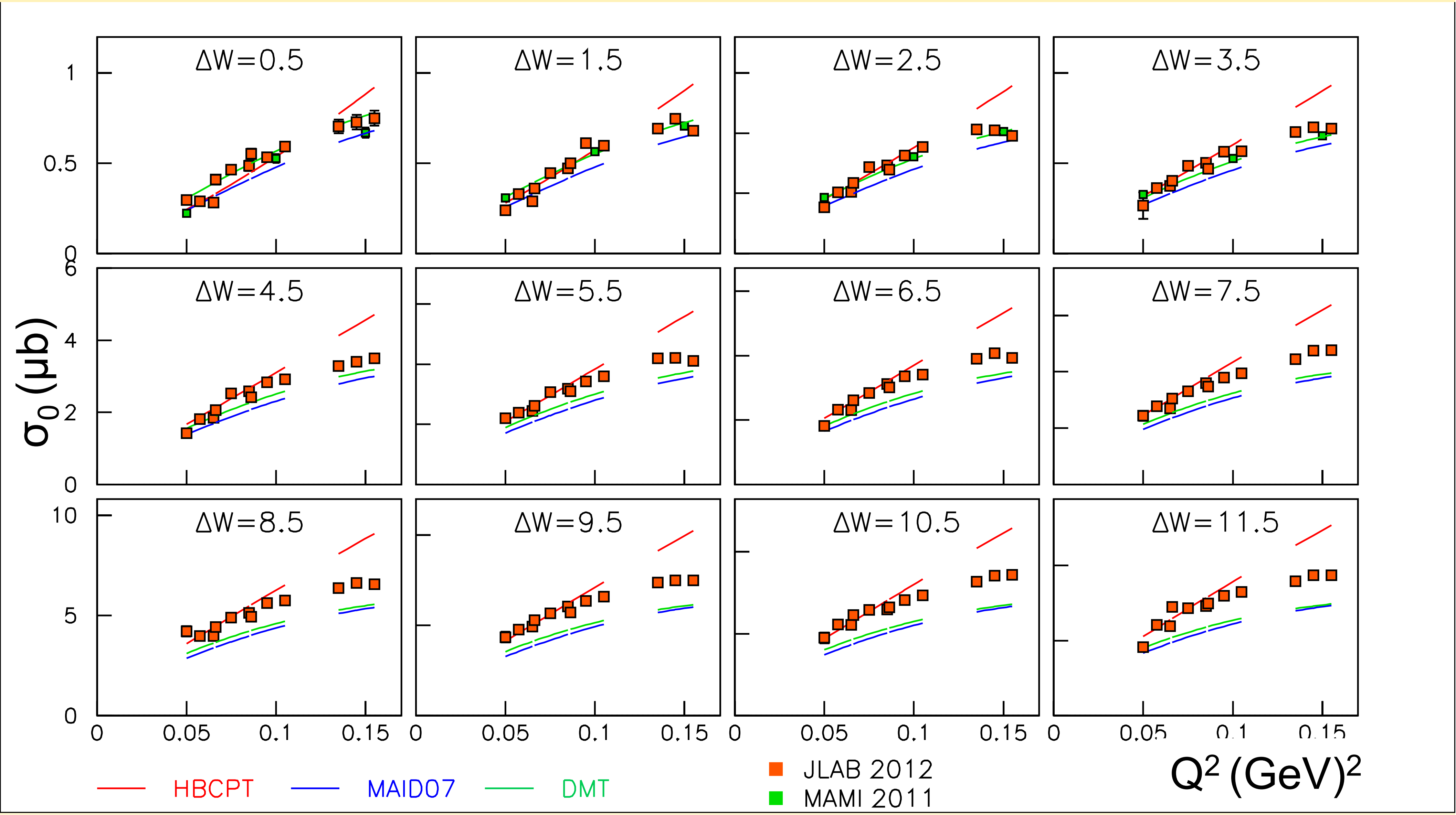

HBChPT
DMT
MAID07

JLAB 2012
MAMI 2011

HBChPT

DMT

MAID07

$A_0 \approx \sigma_{TOT}$

$A_1 \rightarrow \mathrm{Re}(E_{0+}P_1^*)$ dominates

$A_2 \rightarrow |P_2|^2 + |P_3|^2$ p-waves

JLAB 2012

MAMI 2011

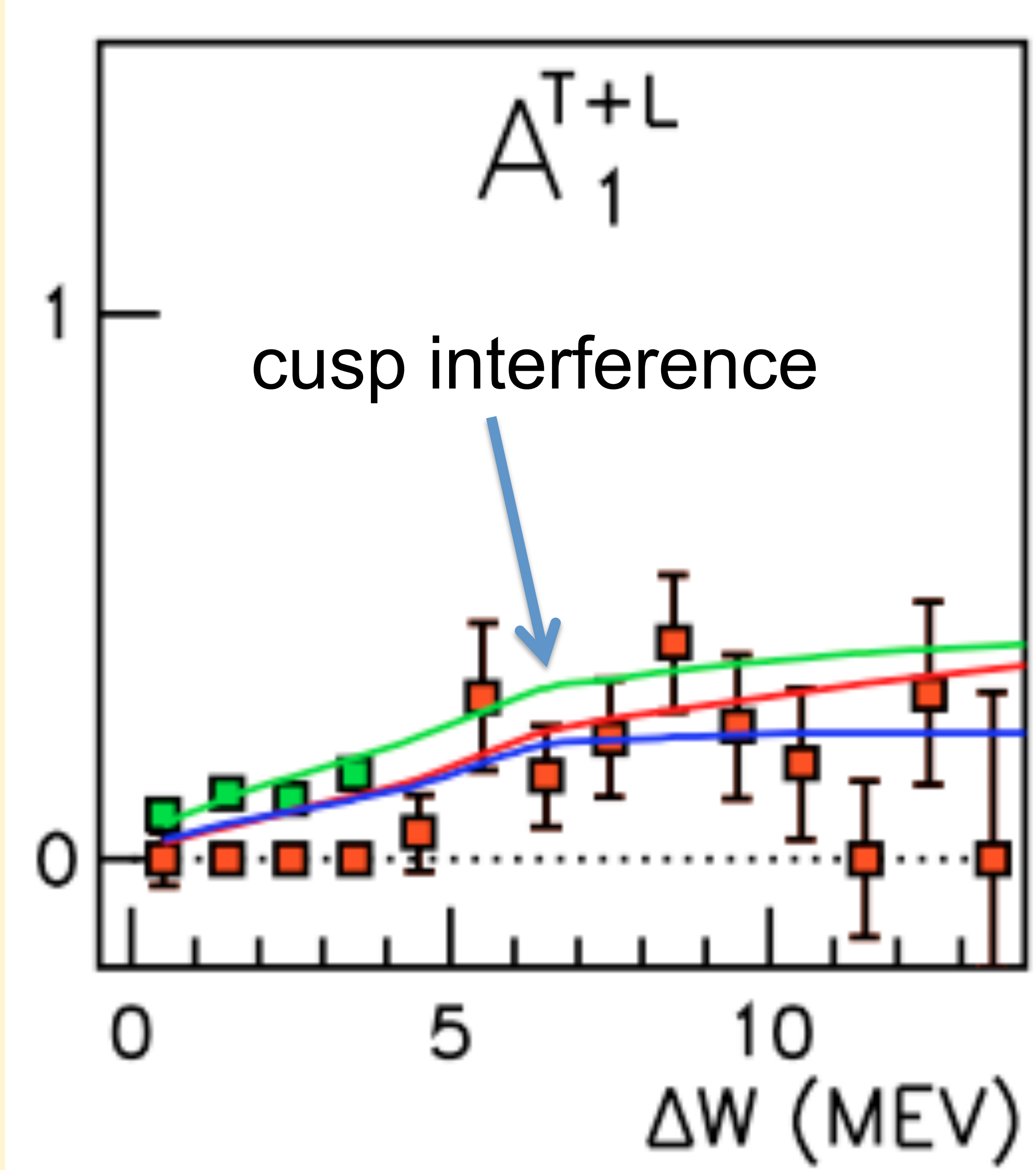

Jefferson Lab

this latter value as a measure for the theoretical uncertainty of our calculations. For the S-waves, we have a priori two new counter terms at order q^4,

$$E(k^2)^{ct} = eM_\pi\{(a_1+a_2)M_\pi^2 - a_3k^2]$$
$$L(k^2)^{ct} = eM_\pi\{(a_1+a_2)M_\pi^2 - a_3k^2 + a4(M_\pi^2 - k^2)\} \quad (40)$$

so that $L(k^2) - E(k^2) \sim (1+\rho)$. However, as proven in Appendix A, in the soft-pion limit one can show that

$$a_3 + a_4 = 0\,, \quad (41)$$

and thus there is only one LEC and furthermore a strong correlation between $E(k^2)^{\rm ct}$ and $L(k^2)^{\rm ct}$ at order q^4. The low-energy constant a_3 will be treated as a free parameter and pinned down by a fit to the available differential cross section data at $k^2 = -0.1$ GeV^2. It turns out, however, that with a k^2-independent $L^{\rm ct}(k^2)$, i.e. with the k^2 dependence of $L(k^2)$ coming solely from the Born and loop graphs, one is not able to fit the existing data. We therefore have to include the first corrections to the soft-pion constraint (41) away from the chiral limit. This induces a term of the type

$$L_{0+}^{ct} = -eM_\pi^2 k^2 a_5 \quad (42)$$

which arises from terms in the Lagrangian $\mathcal{L}_{\pi N}^{(5)}$ and is thus of higher order. This is

From V. Bernard et al., Nucl Phys A607 (1996) 379

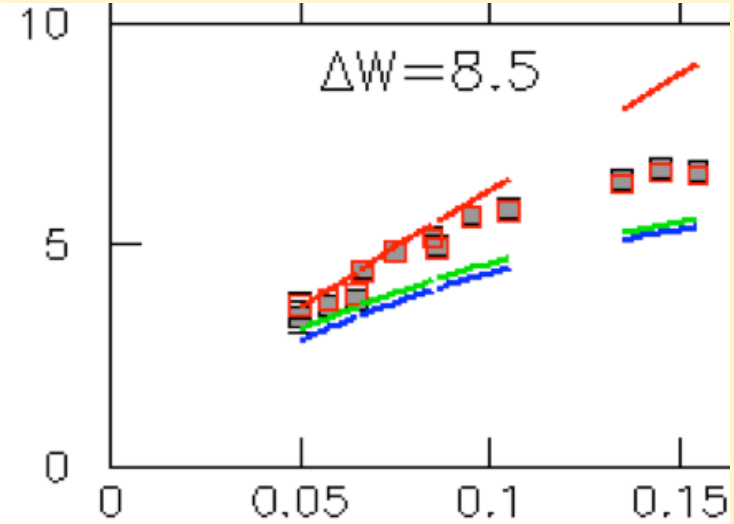

HBChPT LEC (1996)

b_p = 13.0

a_1+a_2 = 7.84

a_3 = -1.37

a_4 = - 0.22

a_5 = 0

Substantial increases in a4 and a5 LECs required to describe Q^2 dependence of our data above Q^2=0.1.

Jefferson Lab

ΔW (MeV) Dependence of A^{LT}

A^{LT}

- HBChPT
- DMT
- MAID07

- JLAB 2012
- MAMI 2011

$A_0 \rightarrow \mathrm{Re}(L_{0+} P_2^*)$ dominates

$A_1 \rightarrow$ Weak longitudinal p-waves

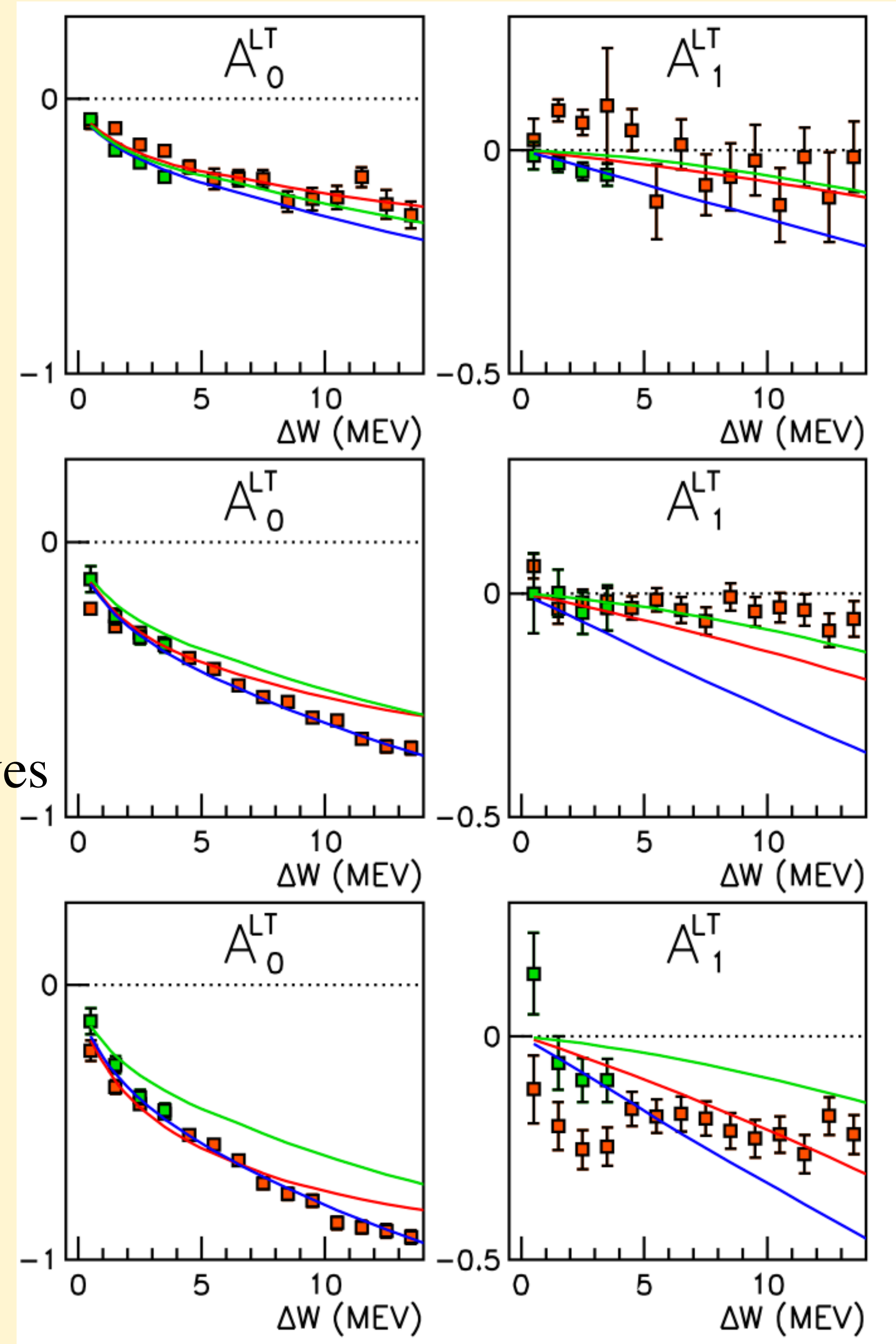

Q^2=0.05

Q^2=0.10

Q^2=0.15

Jefferson Lab

Q^2 Dependence of A_0^{LT} from 0.5 to 11.5 MeV

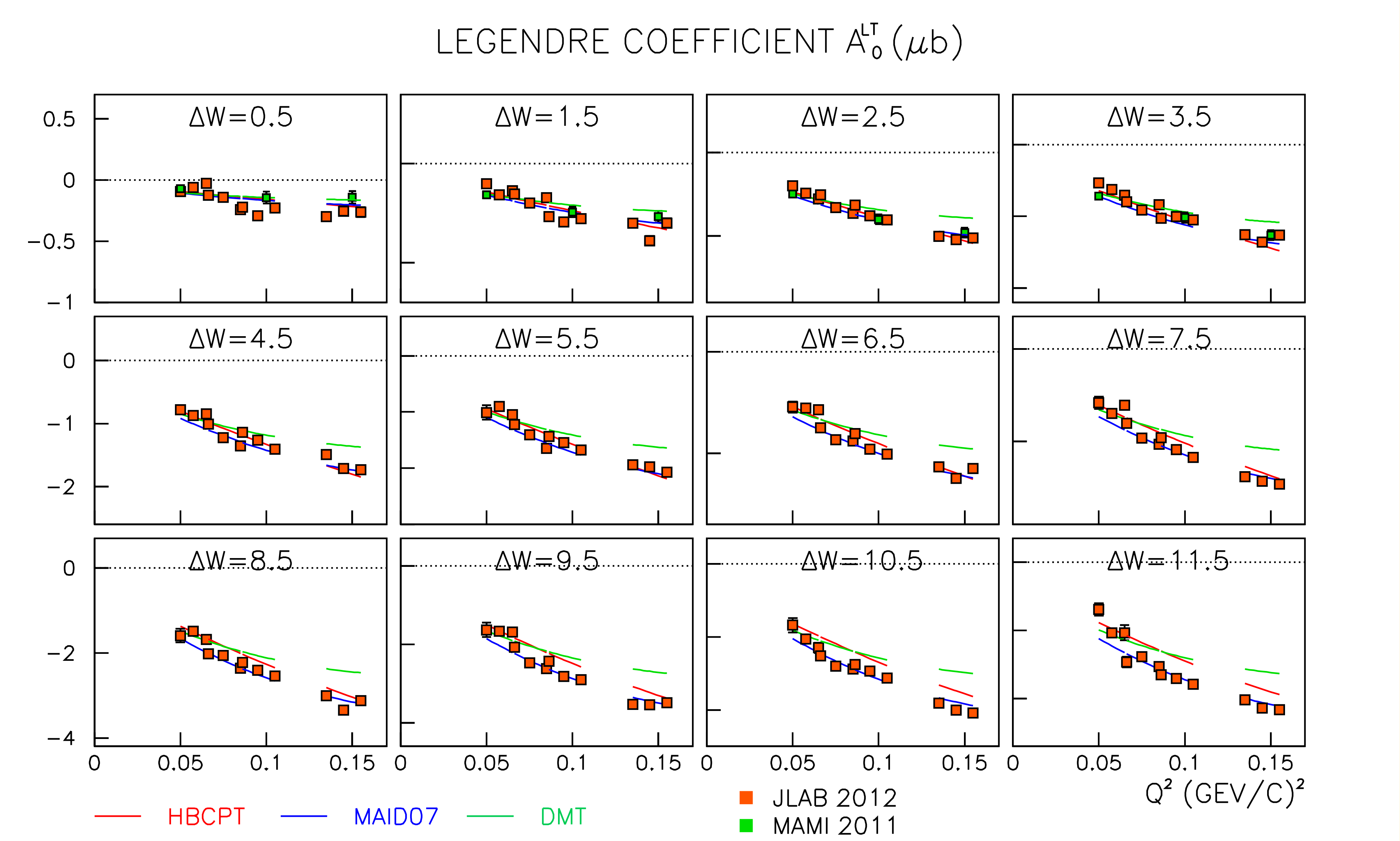

Jefferson Lab

Beam Asymmetry Sensitive to Imaginary Part of ($L_{0+}P^*_2+E_{0+}P^*_5$)

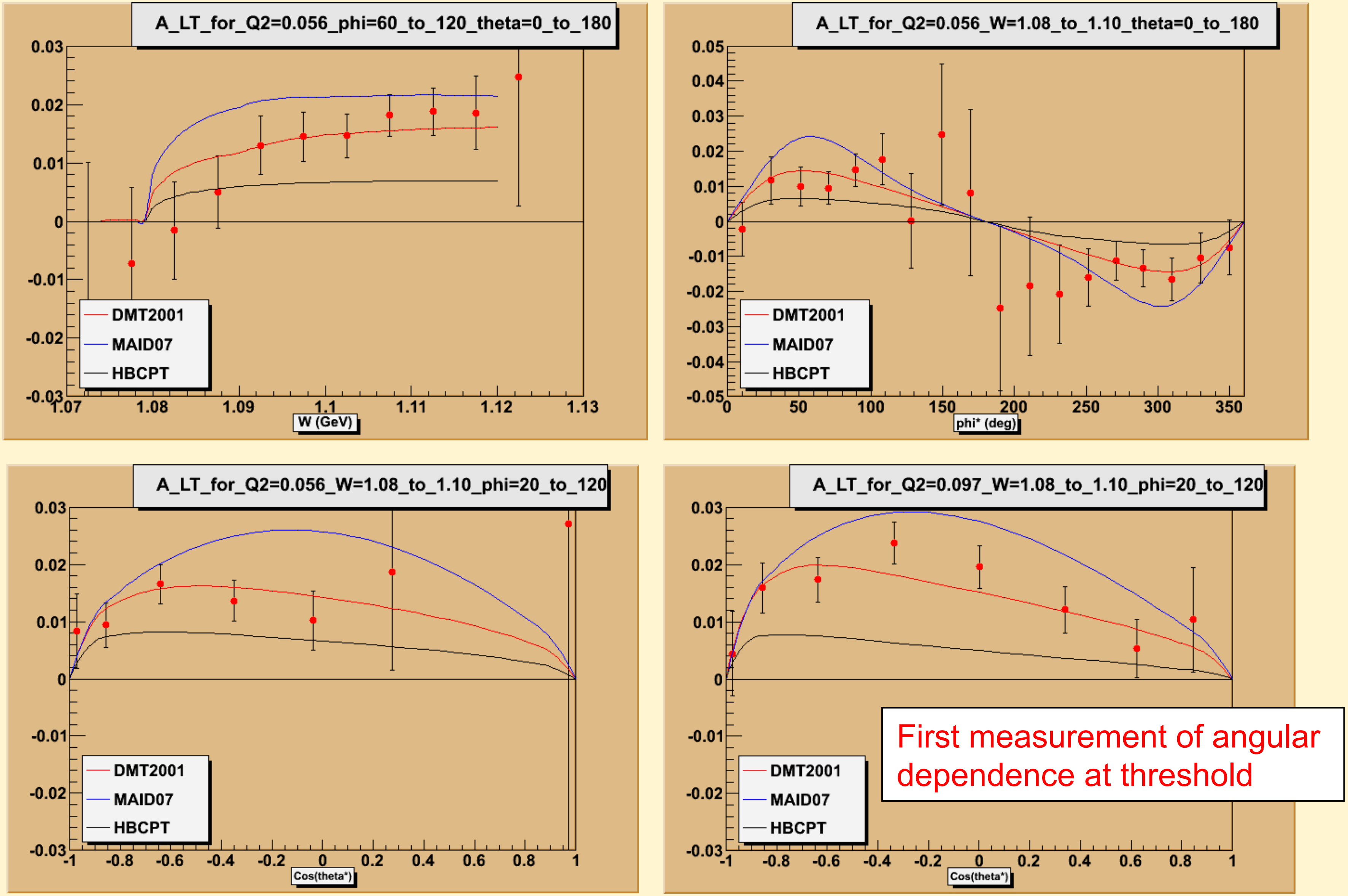

Note color code change

$$A_{LT'} = \frac{1}{P_e}\frac{(N^+ - N^-)}{(N^+ + N^-)}$$

Jefferson Lab

Systematic Effects Studied

- Electron Energy calibration
- BigBite wire chambers, optics, calibration
- Light attenuation along scintillation paddles
- BigBite magnetic field , fringe fields, clamp effects
- BigBite acceptance and simulations using GEANT3
- Bin Migration, Straggling and Energy Loss Corrections
- Time of flight and background due to accidentals
- Missing mass spectrum and window background subtraction from quasi pion production
- Effects on acceptance determination using DMT/ Maid07

Effect on Total Cross Section Due to Shift in Energy Calibration

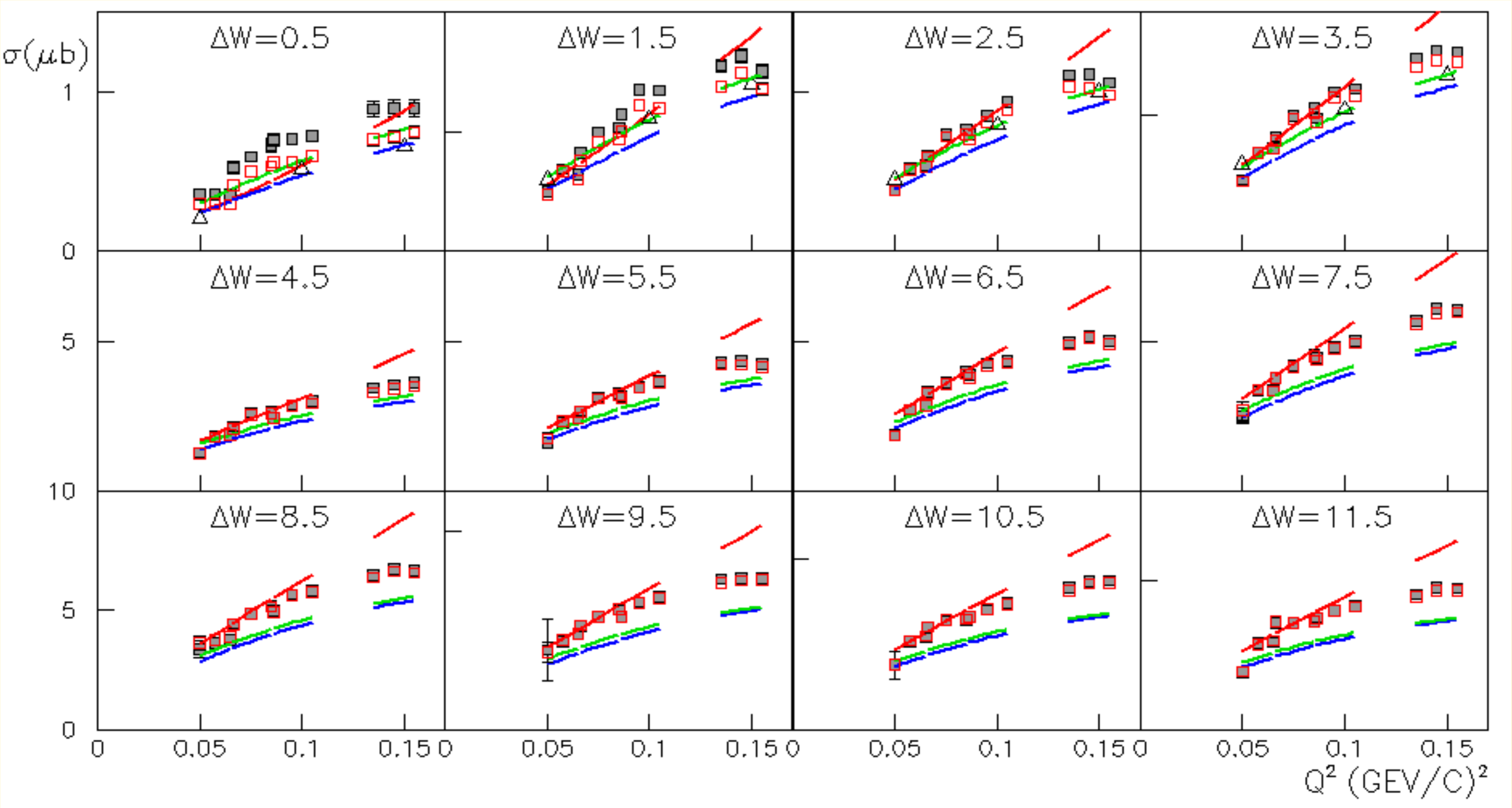

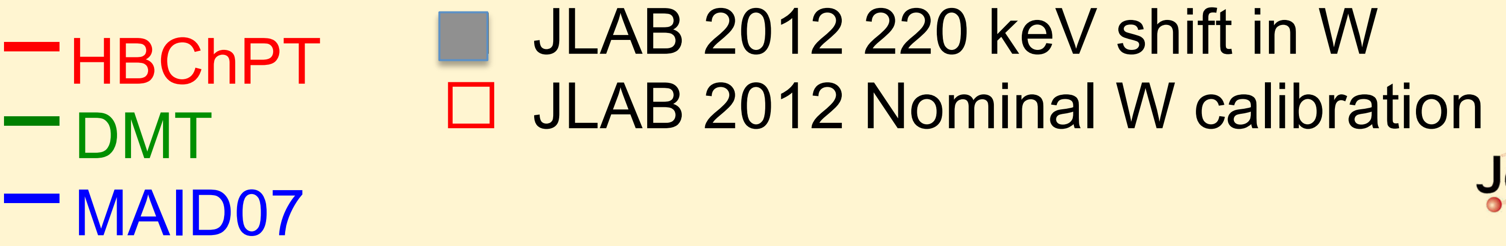

Jefferson Lab

Systematic Error Due to BigBite Acceptance Cuts

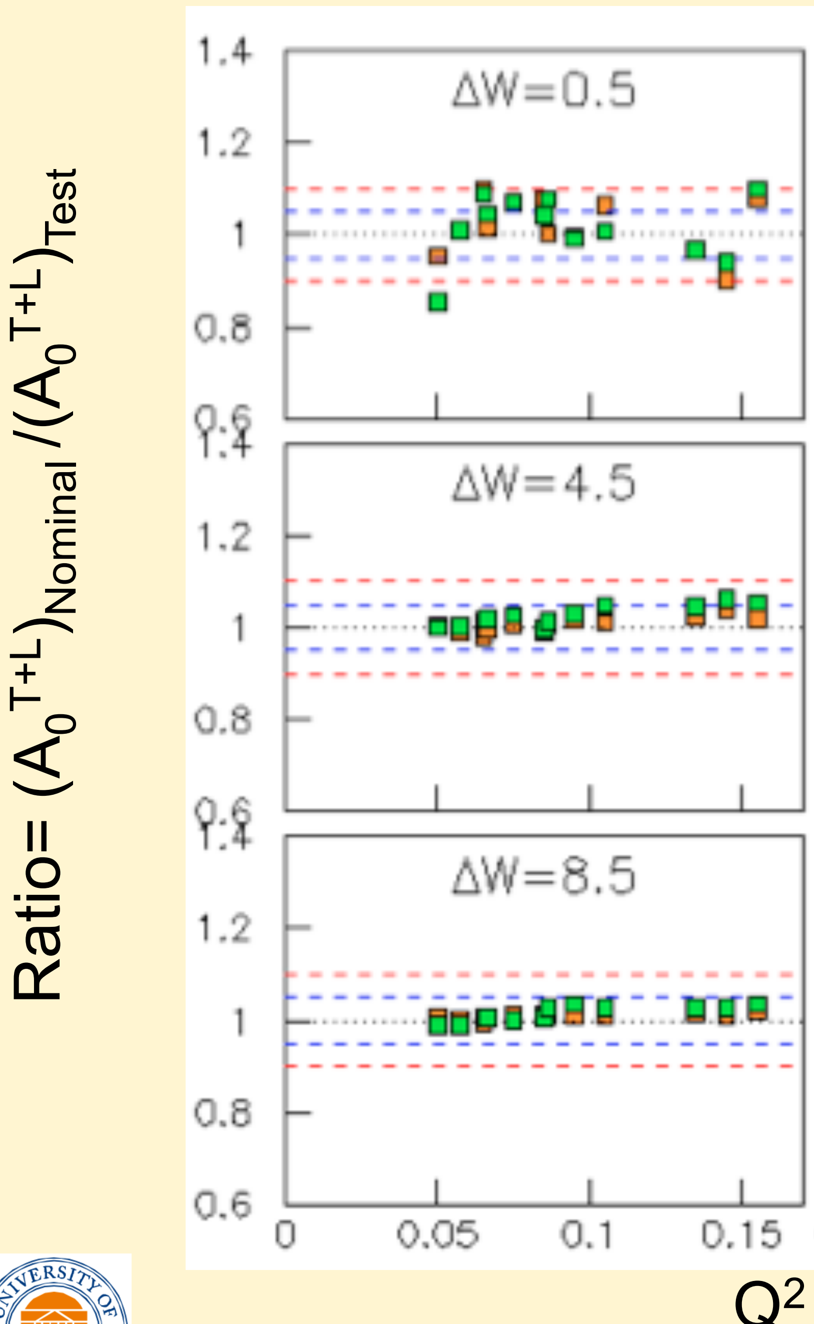

------ +/- 10 % error

------ +/- 5 % error

Orange Fiducial cut x 0.9

Green Fiducial cut x 0.8

Jefferson Lab

Comparison with MAMI 2011 Measurement

JLAB 2012
E=1.192 GeV
ε=0.943

$$\sigma_T + \varepsilon \sigma_L$$

MAMI 2011
E=0.880 GeV
ε=0.882

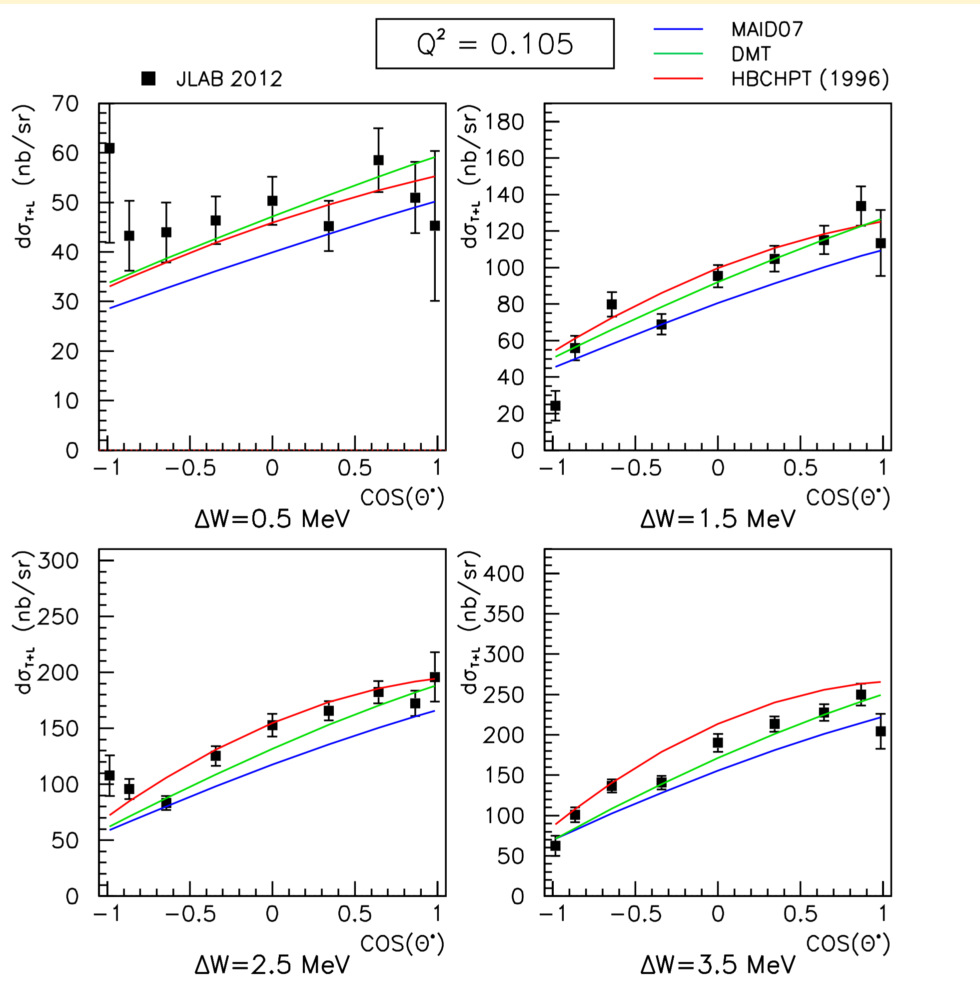

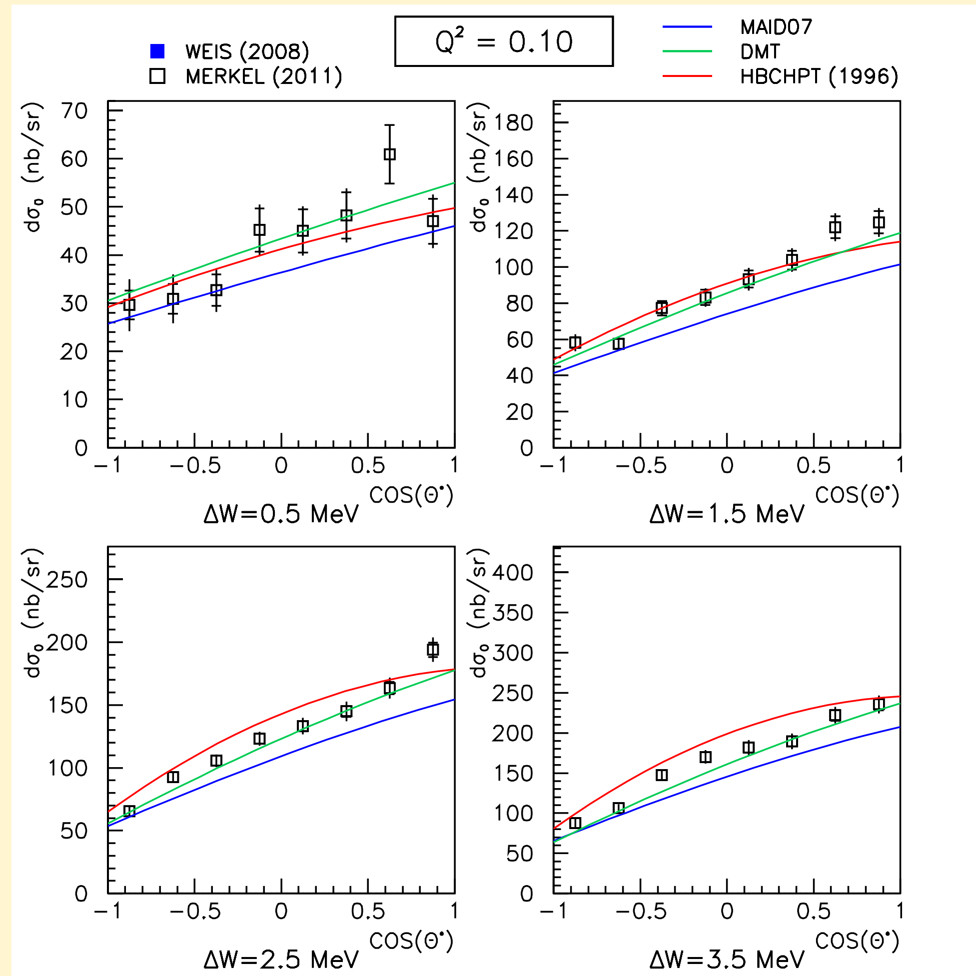

MAMI 2011 H. Merkel et al.,
arXiv:1109.5075v1 [nucl-ex].

Jefferson Lab

Comparison with MAMI 2011 Measurement σ_{LT}

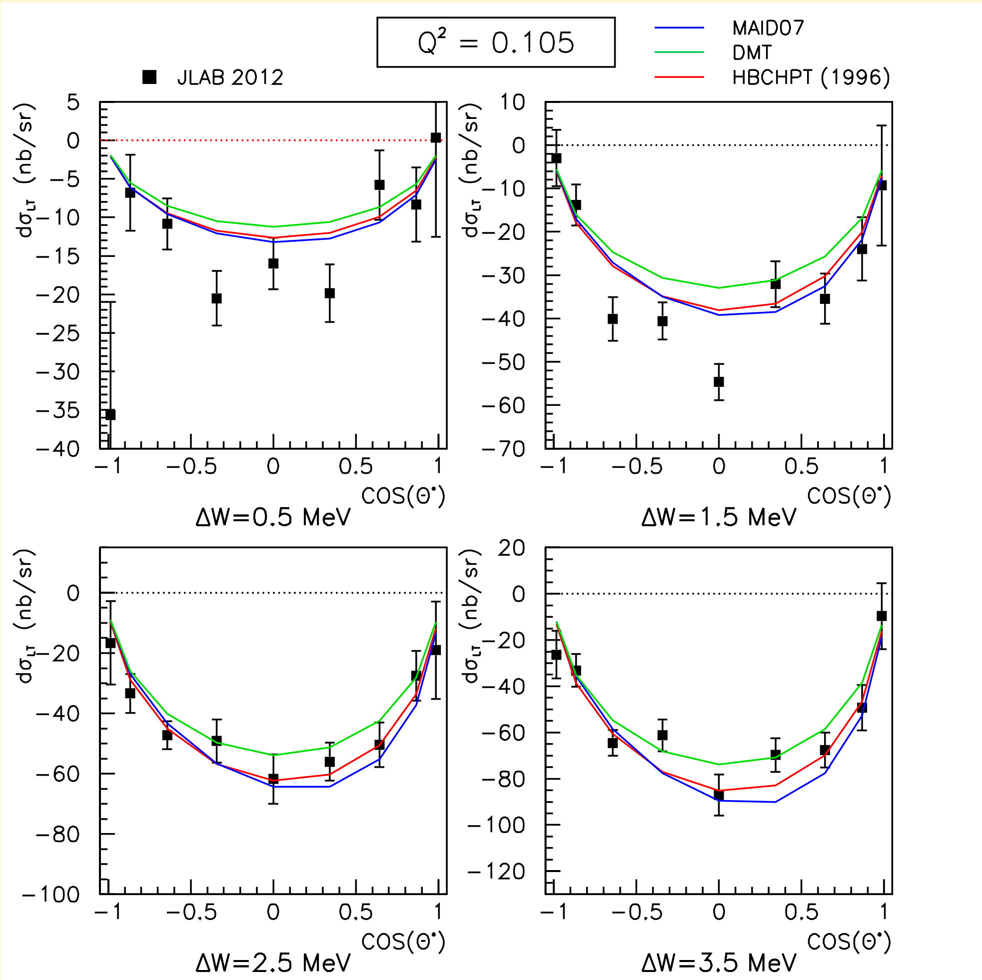

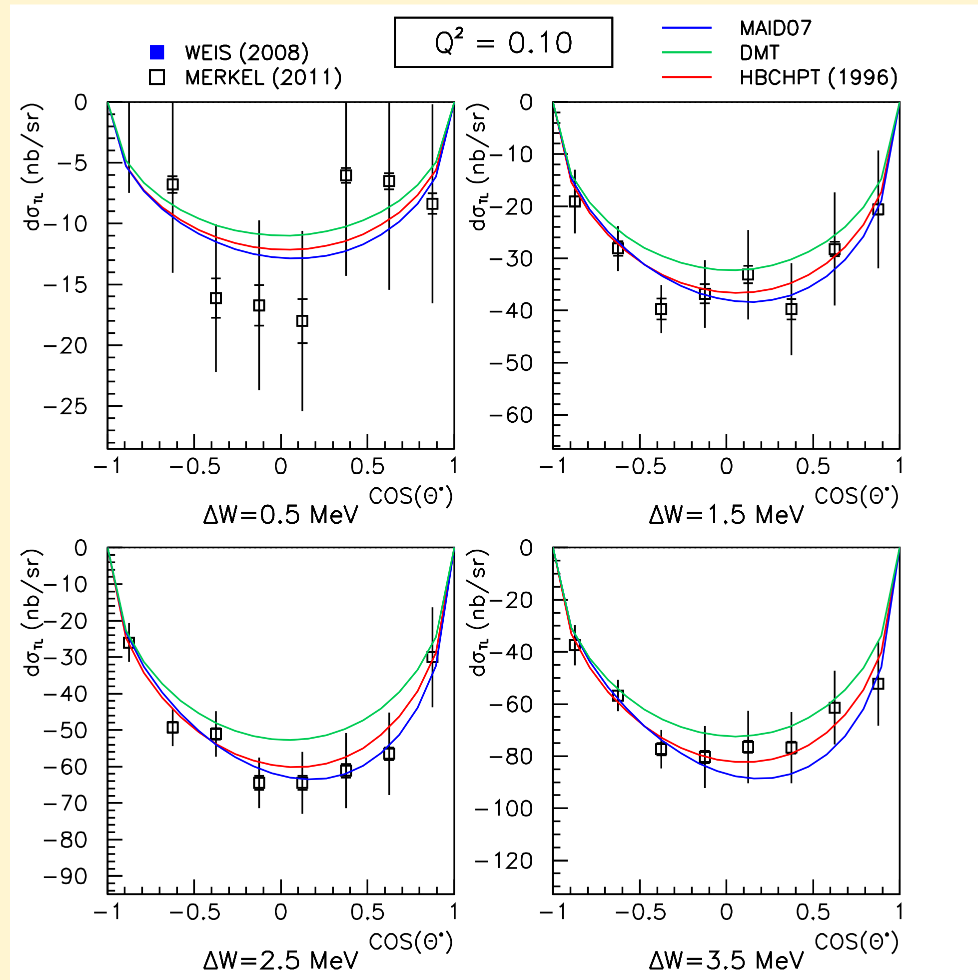

JLAB 2012
E=1.192 GeV

MAMI 2011
E=0.880 GeV

Jefferson Lab

Conclusions E04-007

- $Q^2 < 0.10$ $(GeV/c)^2$ JLab2012 data for σ_0 and σ_{LT} agrees with HBChPT and the new MAMI data in the range $0.5 < \Delta W < 4.0$ MeV

- $Q^2 > 0.1$ $(GeV/c)^2$ JLab2012 data for σ_0 falls off faster in Q^2 than the prediction by HBChPT. May require new LEC constant a_5 and higher order calculation.

- JLab2012 data σ_{TT} is in clear disagreement with ChPT and gets worse with increasing Q^2 and W. This term is sensitive to the P_3 LEC counter term $b_{p.}$

- Further studies are underway to extend results up to 30 MeV and up to $Q^2 = 0.5$ $(GeV/c)^2$. How far can HBChPT be successful?

- Continue to evaluate systematic effects which can influence the threshold cross sections. Make multipole analysis.

Jefferson Lab